bluecoast
CONSULTING ENGINEERS

Technical Note

To:	ADG Engineers (Aust) - [redacted]
From:	[redacted]
Copy:	
Reference:	P19033-CocosIsland-MoFDesign_DesignWaveClimate_TN4.0.docx
Date:	1 April 2021
Subject:	Cocos (Keeling) Islands – Material offloading facility coastal engineering investigations

1 Introduction

ADG Engineers (ADG) require a coastal engineering investigation to inform the design of a temporary Material Offloading Facility (MOF) on Cocos (Keeling) Islands. The MOF is to be located at the site of the existing boat ramp at Rumah Baru (Figure 1). The study involves two tasks:

- Provide operational (i.e., day-to-day) and design (i.e., extreme) wave climate information that will inform the design of the temporary works. This task is independent of the preferred MOF design.
- An assessment of the impact on coastal processes of the two design options for the MOF structure, where the solid MOF design (option 1) is a solid gravity structure, and the piled MOF design (option 2) is founded on steel piles. The impact assessment considers changes to the local wave climate, lagoon and wave-driven currents, littoral sand transport, shoreline change and wrack accumulation.

2 Wave climate assessment

2.1 Preamble

This section outlines the approach adopted to quantifying the operational (i.e., day-to-day) and design (i.e., extreme) wave climate information that will inform the design of the temporary MOF. The wave climate is determined for a single and predetermined output location nearby the proposed MOF displayed in Figure 1. The local wave climate at the site is primarily influenced by locally generated wind (sea) waves and swell waves generated offshore:

- Wind waves are irregular in frequency and generated by wind blowing across the free surface of the ocean, transferring energy into the water mass through both shear and

pressure effects. The size of the resulting wave is a function of the wind speed, the amount of time the wind blows, and the fetch distance over which the wind acts.

- Swell waves are regular, longer period waves (above 8s) generated by distant weather systems. The swell waves generated offshore then propagate freely across the ocean away from their area of generation.

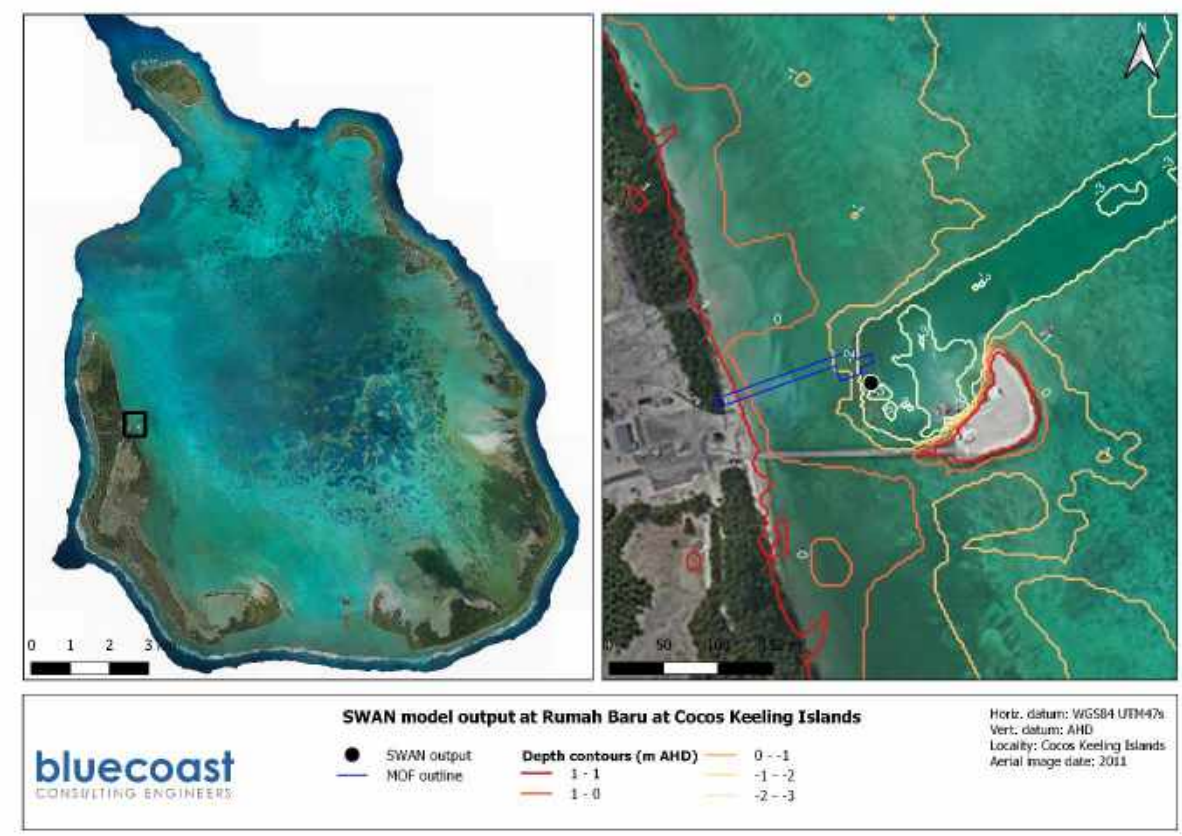

Figure 1: Locations of MOF site and model output locations

2.2 Datasets

The key datasets used to inform the coastal assessment are outlined in Table 1. These datasets are further described in Cocos Keeling Island Coastal Vulnerability Study - Task 2 – Data Review and Gap Analysis (RHDHV, 2018).

Table 1: Overview of key datasets, source and application in the coastal inundation assessment.

Data type	Source	Year
Wave	CAWCR hindcast model extraction point: [-12.4°, 96.8°]	January 1979 to November 2019

Data type	Source	Year
Winds	Bureau of Meteorology (BoM) anemometer (airport)	2006 to 2019
Water levels	BoM tide gauge (Home Island jetty)	1992 to 2019
Bathymetry and topography	Topographic Digital Elevation Model LiDAR (1m resolution)	2011
	Bathymetric LiDAR (~25m resolution)	2012
	GEBCO offshore bathymetry	2014

2.3 Model setup

Deltares' D-Waves spectral wave model was used for this study. D-Waves utilises the widely adopted third generation Simulating WAves Nearshore (SWAN) engine to simulate wave propagation, wave generation by wind, non-linear wave-wave interactions and dissipation.

The spectral wave model was used to determine the nearshore wave climate at the study site by propagate sea and swell waves from global wave model extraction locations inshore to the nearshore areas of CKI. The wave model adopted for this study was previously calibrated in the Cocos (Keeling) Island – Coastal Vulnerability Assessment (CVA). The model grids outer extents are defined by -11.3° latitude, 95.9° longitude to -12.7° latitude, 97.8° longitude. All models within the study included several nested grids with the following resolutions (see Figure 2):

- Regional domain with 1km spatial resolution
- Transitional domain with 300m resolution
- Nearshore domain with 100m resolution
- West Island domain with 40m resolution.

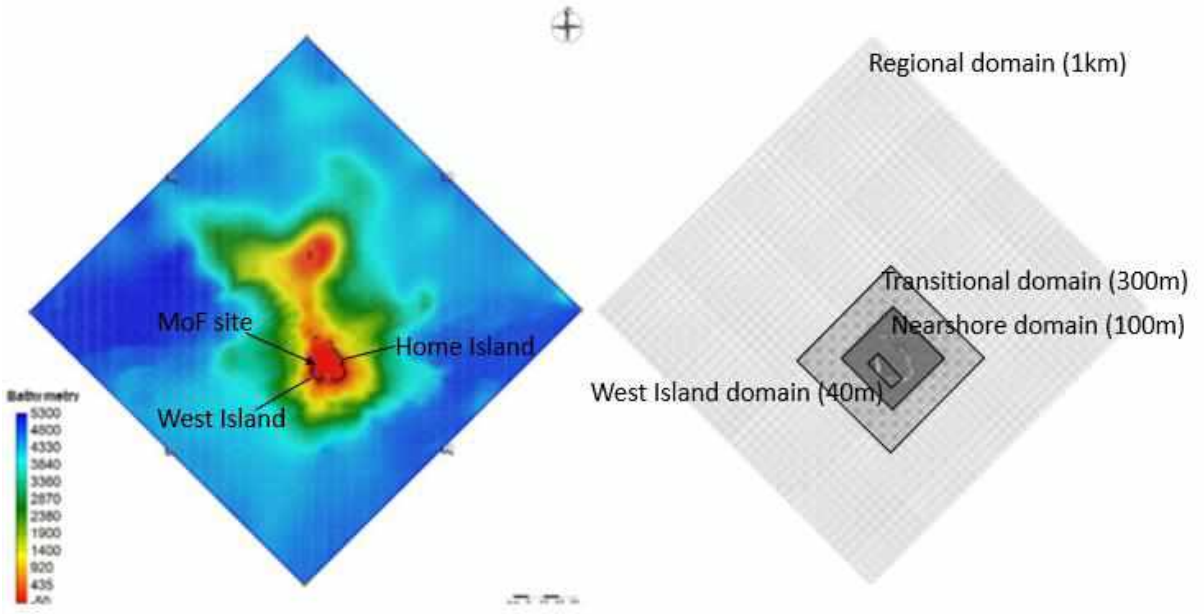

Figure 2: Regional spectral wave model domain extent, bathymetry (left) and four nested grids (right).

2.4 Operational wave climate

To assess the operational (day-to-day) wave climate at the proposed MOF site both locally generated wind (sea) waves and swell waves generated offshore were modelled. Methods and outputs at the predetermined output location are described in the following sections. The water level condition applied to all operational model runs was the average MSL or 0.01mAHD which was extracted from the CKI water level dataset covering 1992 to 2019.

2.4.1 Wind (sea) waves

The locally generated wind waves at the site were modelled using a matrix of stationary model runs with a range of wind speeds and directions forced across the model domains. Figure 3 presents wind roses from the BoM wind station at Cocos Keeling Island (CKI) Airport.

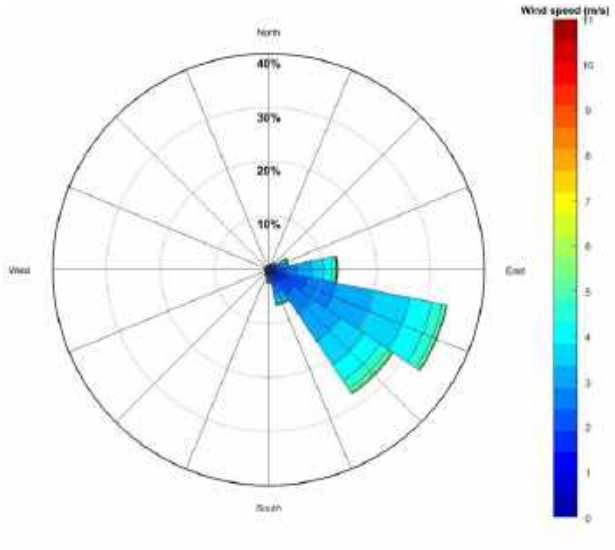

Figure 3: Wind rose from Cocos Keeling Islands Airport for the entire record 2006 to 2019 (source of data: BoM).

The matrix of 184 runs covered the full range of compass directions in 45° intervals and wind speeds from 0m/s to 20m/s at 1 /s intervals. The wave heights, periods and directions were extracted at the output location for the full matrix of runs. The full measurement period from the BoM dataset (2006 – 2019) was used to provide a timeseries of day-to-day wind conditions that could then be transformed into a timeseries of modelled sea waves at the MOF site. The modelled timeseries of wave heights, periods and directions at the MOF site is displayed in Figure 4 and the average seasonal sea wave climate statistics are displayed in Table 2.

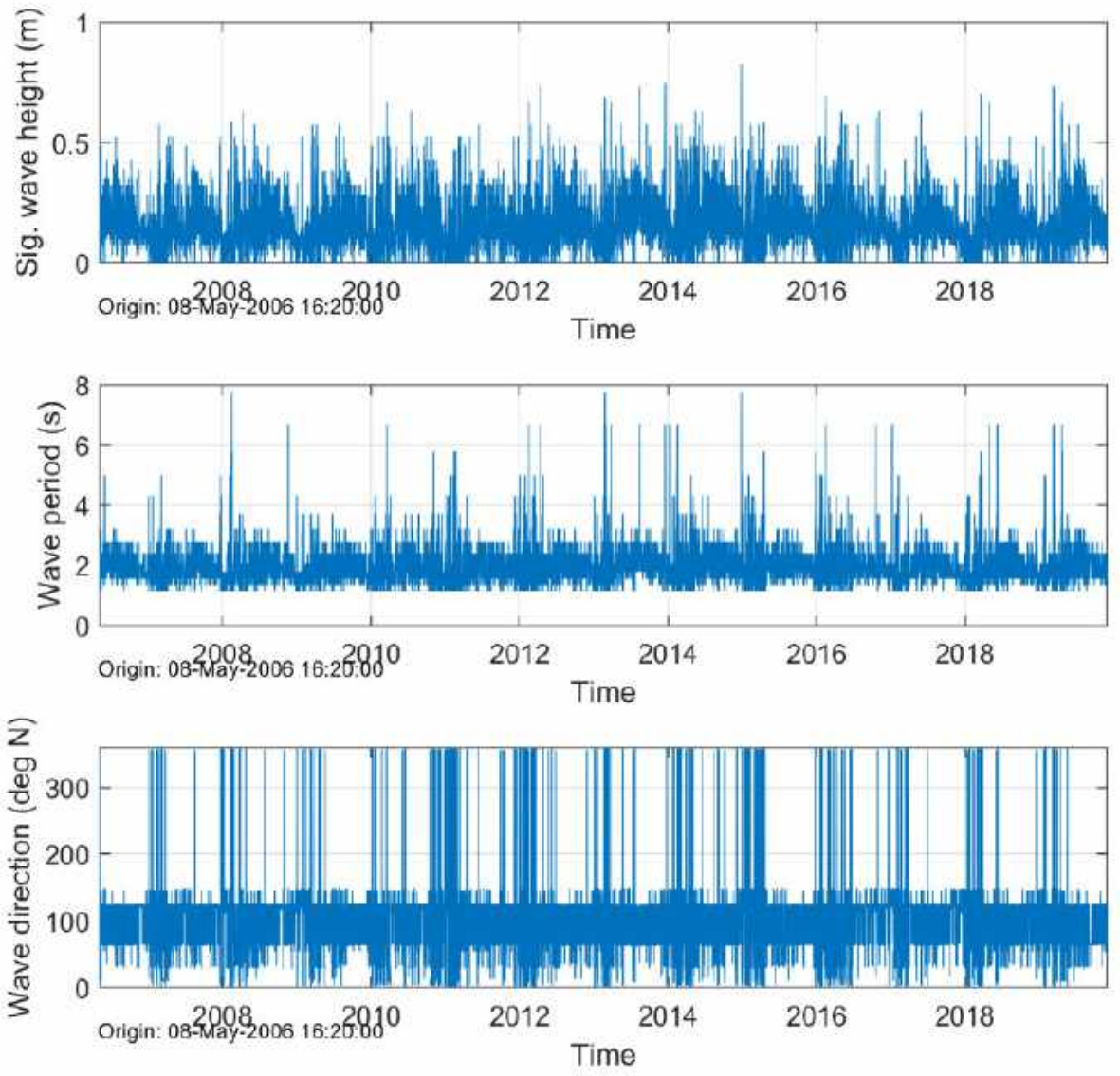

Figure 4: Modelled wind waves for the sea component of the operational wave climate at the MOF site, transformed from the measured winds from Cocos Keeling Islands Airport.

Table 2: Key wave measurement statistics derived from the modelled wind waves for the sea component of the operational wave climate at the MoF site, transformed from the measured winds from Cocos Keeling Islands Airport (2006-2019).

Parameter	Statistic	Long term averages (14-years)				
		All seasons	**Winter**	**Spring**	**Summer**	**Autumn**
Significant wave height (H_s) [m]	Mean	0.14	0.17	0.15	0.11	0.14
	20%ile	0.10	0.12	0.12	0.06	0.08
	50%ile	**0.13**	**0.16**	**0.15**	**0.10**	**0.13**
	75%ile	0.17	0.21	0.17	0.13	0.17
	90%ile	0.22	0.24	0.22	0.17	0.22
	99%ile	0.35	0.35	0.32	0.39	0.39
	99.5%ile	0.39	0.39	0.33	0.43	0.43
	Max	0.83	0.73	0.63	0.83	0.73
Peak wave period (Tm) [s]	Mean	1.9	2.0	1.9	1.8	1.9
	20%ile	1.6	1.8	1.8	1.6	1.6
	50%ile	**1.8**	**2.1**	**1.8**	**1.8**	**1.8**
	75%ile	2.1	2.4	2.1	1.8	2.1
	90%ile	2.4	2.4	2.4	2.1	2.4
	99%ile	3.2	2.8	2.8	4.3	3.2
Mean wave direction (Dp) [˚TN]	Weighted Mean	66	72	78	51	57
	Standard Deviation	34	31	28	39	36

2.4.2 Swell waves

The offshore generated swell waves were modelled using a matrix of stationary model runs with a range of wave period and directions forced from the outer domain boundaries. The boundary conditions were determined from analysis of the CAWCR dataset (1979 to 2019) to cover the full range of wave directions and periods. Figure 5 presents swell wave rose from the CAWCR dataset. A constant wave height of 1m was applied to the matrix of wave periods and directions. Wave heights at the site were then determined based on the coefficient between the offshore wave heights at the boundary and those at the modelled output location.

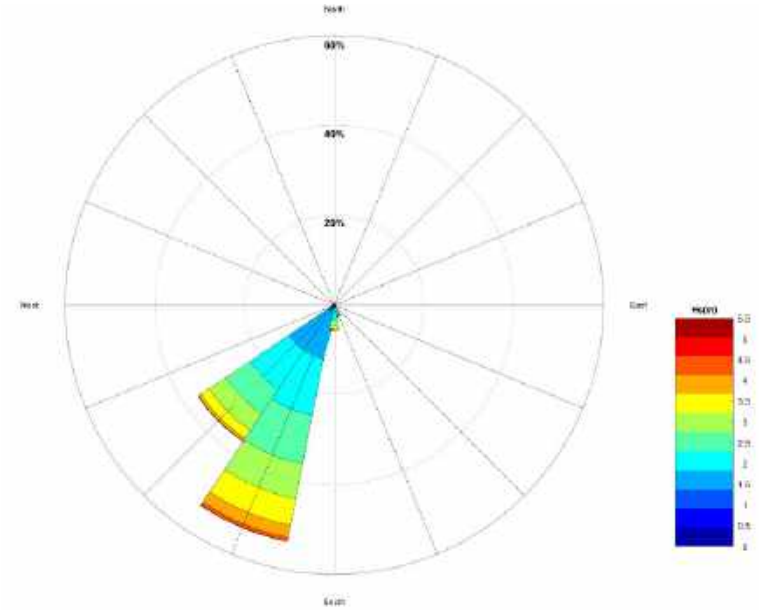

Figure 5: Swell wave rose (Tp > 8s) from CAWCR output from 1997-2019.

The matrix of 80 runs covered the full range of compass directions in 45° intervals and wave periods from 7s to 16s at 1s intervals. The wave heights, periods and directions were extracted at the output location for the full matrix of runs. The full measurement period of swell waves (Tp > 8s) from the CAWCR dataset (1979-2019) was used to provide a timeseries of day-to-day conditions that could then be transformed into a timeseries of modelled swell waves at the MOF site. The modelled timeseries of wave heights at the MOF site is displayed in Figure 6 and the average seasonal offshore generated swell wave climate statistics are displayed in Table 3.

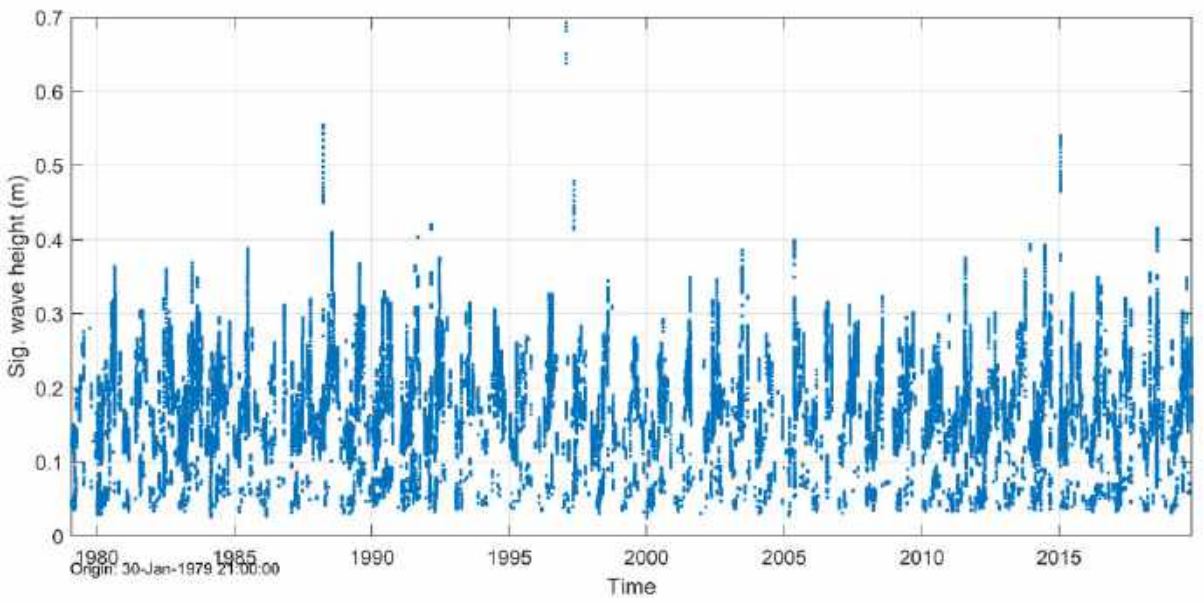

Figure 6: Modelled offshore generated swell waves for the swell component of the operational wave climate at the MOF site, transformed from the CAWCR waves output.

Table 3: Key wave measurement statistics derived from the modelled offshore swell waves for the swell component of the operational wave climate at the MOF site, transformed from the CAWCR waves output (1997-2019).

Parameter	**Statistic**	**Long term averages (41-years)**				
		All seasons	**Winter**	**Spring**	**Summer**	**Autumn**
Significant wave height (H_s) [m]	Mean	0.15	0.19	0.18	0.11	0.13
	20%ile	0.08	0.13	0.11	0.05	0.06
	50%ile	**0.14**	**0.20**	**0.18**	**0.12**	**0.13**
	75%ile	0.20	0.24	0.22	0.14	0.17
	90%ile	0.25	0.28	0.26	0.16	0.21
	99%ile	0.33	0.36	0.32	0.24	0.31
	99.5%ile	0.36	0.37	0.34	0.28	0.35
	Max	0.69	0.42	0.40	0.69	0.55
Wave period (Tm) [s]	Mean	8.8	8.9	8.7	8.6	8.9
	20%ile	7.7	7.7	7.7	7.7	7.7
	50%ile	**8.9**	**8.9**	**8.9**	**8.9**	**8.9**
	75%ile	8.9	8.9	8.9	8.9	8.9
	90%ile	10.4	10.4	10.4	10.4	10.4
	99%ile	12.0	12.0	10.4	12.0	12.0
Mean wave direction (Dp) [˚TN]	Weighted Mean	44	43	43	46	44
	Standard Deviation	3	3	2	4	3

2.4.3 Summary

The modelled operational (day-to-day) wave climate and seasonal statistics at the proposed MOF site are described for the locally generated wind (sea) waves (Table 2) and the offshore generated swell waves (Table 3) and are summarised as:

- Locally generated wind (sea) waves at the MOF site had an annual 50th percentile significant wave height of 0.13m. Consistent with the strength of the trade winds, significant wave heights are slightly larger in winter and spring (50th percentile values of 0.16m and 0.15m, respectively) with lower heights occurring in summer and autumn (50th percentile values of 0.10m and 0.13m, respectively). Locally generated waves are characterised by peak wave periods typically less than 3 seconds. There is a seasonally vary weighted mean wave direction, with winter and spring conditions characterised by waves from 70-80°N while summer and autumn is characterised by slightly more northern wind wave directions (50-60°N).
- Offshore generated swell waves at the MOF site had an annual 50th percentile significant wave height of 0.14m. As with wind generated waves higher significant wave heights also occurring in winter and spring (50th percentile values of 0.20m and 0.18m respectively) than in summer and autumn (50th percentile values of 0.12m and 0.13m respectively). This seasonal variation in swell height at the MOF site is consistent with Indian Ocean swell regime that is more active over the austral winter. Swell waves at the site are characterised by peak wave periods between 8 and 12 seconds, typically from the north-east.

2.5 Design wave climate

To assess the design (extreme) wave climate at the proposed MOF site both locally generated wind (sea) waves and swell waves generated offshore were modelled for the 20-year ARI design level. The locally generated wind wave climate at the site consists of cyclonic and non-cyclonic conditions. Lower return period conditions are governed by non-cyclonic winds while higher return period conditions are governed by cyclonic winds. Methods and outputs at the predetermined output location are described in the following sections.

2.5.1 Sea level

An extreme value analysis (EVA) was undertaken for the 27-year tide gauge record at Home Island (see Table 4). A peak over threshold method was applied for the determination of independent extreme surge events (i.e., minimum 7-days apart). Sensitivity testing of the application of different ARI sea levels was undertaken and it was determined that the 100-yr ARI total water level of 1.16m (AHD) was to be applied to all design wave climate runs.

Table 4: Extreme value analyses results for the Home Island tide gauge data (27-year record).

ARI (years)	Total sea level (m AHD)			Non-tidal residual (m)		
	Estimate	Lower CL*	Upper CL*	Estimate	Lower CL*	Upper CL*
1	**0.98**	0.97	1.00	**0.23**	0.23	0.24
10	**1.09**	1.06	1.11	**0.31**	0.28	0.34
25	**1.12**	1.09	1.15	**0.33**	0.29	0.38
50	**1.14**	1.12	1.17	**0.35**	0.30	0.40
100	**1.16**	1.13	1.19	**0.37**	0.31	0.43

*CL – 98% confidence levels

2.5.2 Non-cyclonic wind (sea) waves

To examine influence of non-cyclonic local winds on the design sea wave climate a directional EVA of the measured winds at the site was undertaken to provide inputs for a matrix of design wind wave runs. Due to the orientation of the MOF site, only winds of north-westerly to southerly orientations were modelled. Table 5 presents the directional EVA of the measured winds at Cocos Keeling Island (CKI) Airport. This measured wind record is approximately 12 years in length and is representative of non-cyclonic conditions. The suite of stationary model runs was forced with the directional non-cyclonic 20-year ARI wind speeds across the model domains.

The wave heights, periods and directions were extracted at the output location for the full matrix of runs in Table 6. Spatial maps of the significant wave heights modelled over the two highest resolution domains are provided for the northerly, easterly and south-easterly wind directions in Figure 7.

Table 5: Directional extreme value analyses result of the 20-year ARI wind speeds for the BoM CKI Airport data (2006-2019) with the selected modelled cases identified (bold).

Wind directional bins	Wind speeds (m/s)		
	Estimate	Lower CL*	Upper CL*
Omni	18.5	16.4	20.6
N	14.3	13.0	15.6
NE	17.7	15.0	20.4
E	17.1	15.7	18.5
SE	16.0	14.7	17.3
S	14.5	13.2	15.8
NW	13.4	11.6	15.1

*CL – 98% confidence levels

Table 6: Modelled design wind waves at the MOF output with the maximum design wind (sea) waves in bold

Input 20yr ARI winds		Modelled wave parameters		
Wind direction	**Wind speed**	**H sig. (m)**	**Peak period (s)**	**Mean direction (deg)**
N	**14.3**	**1.13**	**6.7**	**26**
NE	17.7	1.09	7.7	35
E	17.1	0.64	3.7	58
SE	16.0	0.40	2.8	121
S	14.5	0.30	2.4	152
NW	13.4	0.82	5.8	20

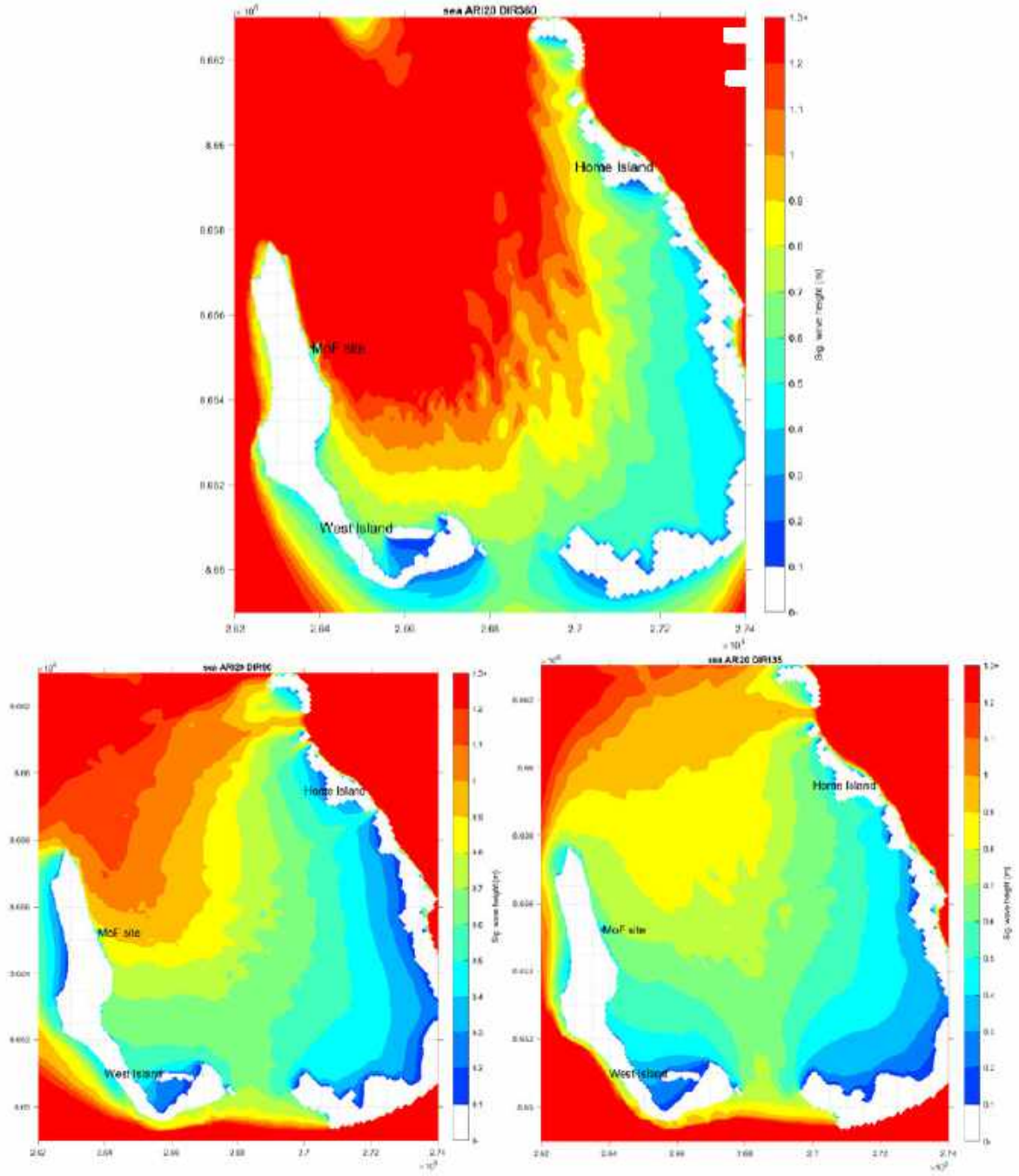

*Figure 7: Modelled 20yr ARI significant wave heights (wind wave – sea only) at Cocos Keeling Islands from the 20yr ARI northerly (top), easterly (bottom left) and south-easterly (bottom right) winds and the MOF site (black *).*

2.5.3 Cyclonic wind waves

While it is rare for a destructive tropical cyclone to track within proximity to CKI. It is therefore necessary to assess cyclonic wind waves using an alternative approach that does not rely on local wind measurements. A 1,000-year synthetic Tropical Cyclone dataset developed as part of the Cocos (Keeling) Island – Coastal Vulnerability Assessment (CVA) was used. Figure 8 provides a plot that compare extreme non-cyclonic (blue) and cyclonic wind speeds. Based on this plot above the 8-year ARI maximum extreme wind speeds are governed by cyclonic conditions. Also, the cyclonic wind speeds are estimated as 30.5m/s and 36m/s for the 20-year and 50-year ARI, respectively wind speed of.

Five model runs were undertaken for cyclonic wind speeds as defined in Table 7. The 20-year and 50-year design winds were applied to northeast (noted as 35°N in Cocos (Keeling) Island – Coastal Vulnerability Assessment (CVA)) and eastly design events with an additional case for the 20-year cyclonic wind speeds from the north to define a rare yet more severe case as northerly events have the longest fetch at the site. The wave heights, periods and directions were extracted at the output location for the two runs in Table 7.

The 50-year ARI cyclonic condition from a northerly direction has not been provided as it is difficult to accurately estimate this condition. It is likely to be beyond the capacity of the temporary structure to affordably accommodate a northerly cyclonic event. Active and project specific forecasting of cyclones should be considered during cyclones seasons over key construction periods.

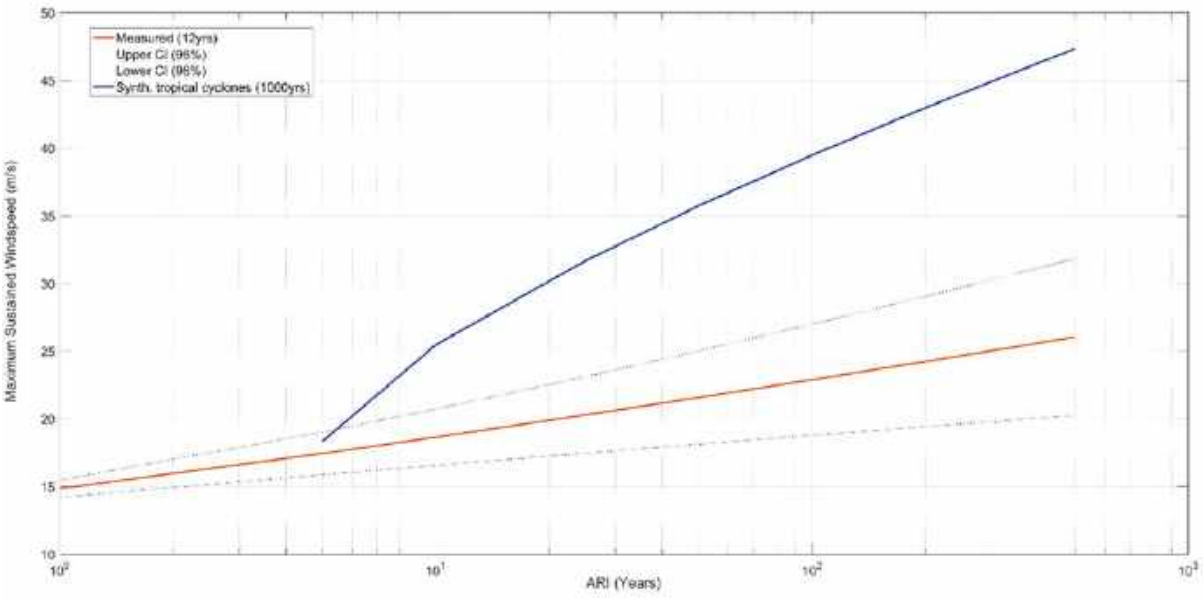

Figure 8: Results from the EVA for measured wind speeds at CKI and the 1,000-year synthetic tropical cyclone record (all directions) at CKI.

Table 7: Modelled wind waves from the cyclonic design winds at the MOF output

	Input cyclonic winds		Modelled wave parameters		
ARI	**Wind direction**	**Wind speed**	**H sig. (m)**	**Peak period (s)**	**Mean direction (deg)**
20yr	N - 360°N	30.5	1.36	10.4	29
20yr	NE - 35°N	30.5	1.28	8.2	39
20yr	E - 90°N	30.5	1.06	4.3	62
50yr	NE 35°N	36.0	1.30	4.3	43
50yr	E – 90°N	36.0	1.13	5.0	65

2.5.4 Offshore swell waves

To examine influence of the offshore generated swell wave component on the design wave climate, a directional EVA was undertaken for the swell wave component at the offshore extraction point of the CAWCR data. Table 8 presents the directional EVA (and Figure 9 the omni directional analysis) of the swell waves at the CAWCR output location along with the associated wave period which was determined from the average of the top five peak events in each directional EVA. It is to be noted that the spatial and temporal resolution of the CAWCR wave models do not allow an accurate representation of tropical cyclones and associated wave conditions. The EVA provided inputs for a matrix of design swell wave runs. There was insufficient data to provide the 20-year ARI values for the swell waves with north to east directions and thus not modelled in the matrix. This is because these swell wave directions are rare at Cocos (keeling) Islands as reflected in the CAWCR wave data. The suite of stationary model runs was forced at the offshore boundaries with the directional 20-year ARI wave heights and associated wave periods across the model domains.

The wave heights, periods and directions were extracted at the output location for the full matrix of runs in **Error! Reference source not found.**. Spatial maps of the significant wave h eights modelled over the two highest resolution domains are provided for the northerly, easterly and south-easterly wind directions in Figure 10.

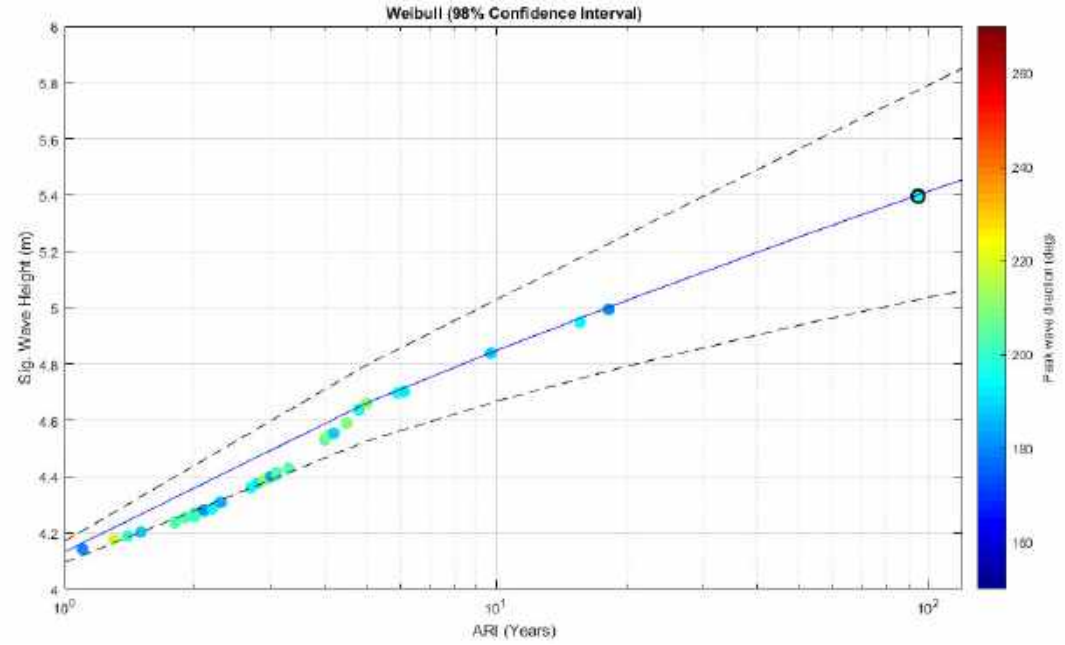

Figure 9: Average recurrence interval (ARI) offshore swell wave heights for CKI (note: tropical cyclones not accurately included). The coloured dots show the analysis events and associated wave directions. The black circled dot (top panel) represents the July 2018 swell event.

Table 8: Directional extreme value analyses result of the 20-year ARI swell waves for the CAWCR dataset (1979 - 2019) with the selected modelled cases identified (bold).

Wind directional bins	**Wave heights (m)**			**Avg. wave period (s) for the 20yr ARI wave height**
	Estimate	Lower CL*	Upper CL*	
Omni	5.4	5.1	5.6	9.6
SE	5.8	5.6	6.0	9.6
S	5.3	5.0	5.6	9.4
SW	5.3	5.0	5.5	9.2
W	3.3	2.4	4.1	9.3
NW	4.1	3.8	4.4	8.1

*CL – 98% confidence levels

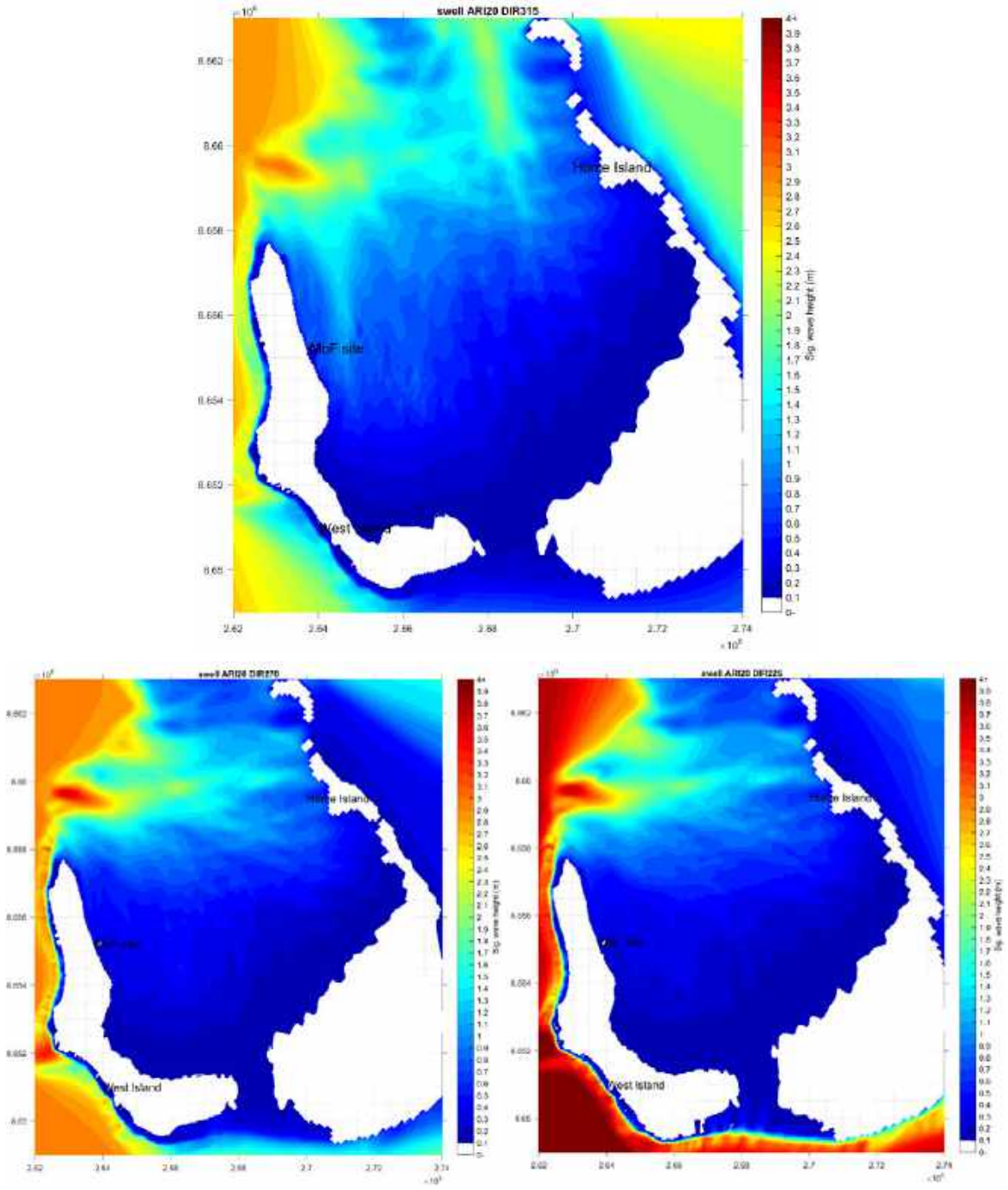

*Figure 10: Modelled 20yr ARI significant wave heights (swell wave only) at Cocos Keeling Islands from the 20yr ARI waves from the northwest (top), west (bottom left), and southwest (bottom right) and the MOF site (black *)*

Table 9: Modelled design swell waves at the MOF output with the maximum design swell waves in bold.

Input 20yr ARI swell waves			Modelled wave parameters		
Direction	**Wave height (m)**	**Period (s)**	**H sig. (m)**	**Peak period (s)**	**Mean direction (deg)**
SE	5.8	9.6	0.17	10.4	33
S	5.3	9.4	0.22	10.4	30
SW	5.3	9.2	0.34	12.0	33
W	3.3	9.3	0.40	10.4	36
NW	**4.1**	**8.1**	**0.70**	**8.9**	**40**

2.5.5 Summary

The maximum modelled 20-year ARI design waves (extreme) at the proposed MOF site were:

- The maximum modelled 20yr ARI sea waves were from local wind forcing were those associated with northerly winds. The waves generated at the MOF site had a significant wave height of 1.13m, a 6.7s peak wave period and was from a direction of 26°N.
- Modelled sea waves during the design tropical cyclone event (NE) for the 20yr ARI wind speed had a significant wave height of 1.28m, a from a direction of 39°N. The largest waves for the 20year design tropical cyclone cases were from a northerly wind direction as this has the longest fetch, generating offshore swell waves of larger periods (10.4s) which propagated to the site. The 50year design tropical cyclone case from the NE produced a significant wave height of 1.3m with a 4.3s.
- The maximum modelled 20yr ARI swell waves were from offshore swell waves from the northwest and generated waves with a significant wave height of 0.7m, an 8.9s peak wave period and 40°N wave direction at the MOF site.

3 Coastal processes assessment

3.1 Preamble

An assessment of the impact on coastal processes of two potential MOF design was completed. The impact assessment considers changes to the local wave climate, lagoon and wave-driven currents, littoral sand transport, shoreline change and wrack accumulation. Changes to the key physical processes and seasonality will be considered in this impact assessment. The assessment of coastal processes will focus on ambient (i.e. typical and high-energy annual) conditions, rather than cyclonic conditions. This is because morphological change in response to the MOF structure will be governed by ambient conditions.

3.2 Site and design information

3.2.1 Project site

The proposed MOF facility is to be located at Rumah Baru (see Figure 1), on the eastern (lagoon) shores of West Island. The Rumah Baru port facility was constructed in 2011. The terminal provides for ferry services to Home Island and Direction Island and is currently the only point of entry for containers and heavy equipment to West Island. The ferry terminal comprises an island terminal (reclaimed) with a piled jetty connecting it to shore. The island terminal is constructed from concrete with a geotextile sand container revetment and has a solid concrete deck. A dredged channel is located to the north of the terminal. A recreational boat ramp was also constructed at the same time as the terminal and requires semi regular excavation works to the north and south to prevent siltation (Figure 11).

Located on the lagoon facing shoreline Rumah Baru is a relatively low energy wave environment. The shoreline comprises of a narrow sandy beach backed by dense vegetation (Cocos palms). The nearshore area is shallow to approximately 1m AHD out to the end of the proposed MOF and Rumah Baru wharf, 2m at 500 m from the shoreline, and 3m inside the dredged channel (Figure 12). The area is covered by extensive seagrass beds offshore which act to dissipate wave energy (RHDHV, 2018b). Cocos (Keeling) Islands are an extremely diverse and high value marine habitat and Rumah Baru is no exception. Turtles are often seen in this area, being attracted by the seagrass beds. As well as changes to shoreline dynamics, any changes to current as a result of the MOF structure will have the possibility of disturbing the marine life and seagrass beds.

Figure 11: Boat ramp and Rumah Baru ferry terminal (south facing) on the lagoon side of West Island in February 2019 (top left and top right), areas to the north and south of boat ramp where sand is removed (bottom left), and location of main features at Rumah Baru (bottom right).

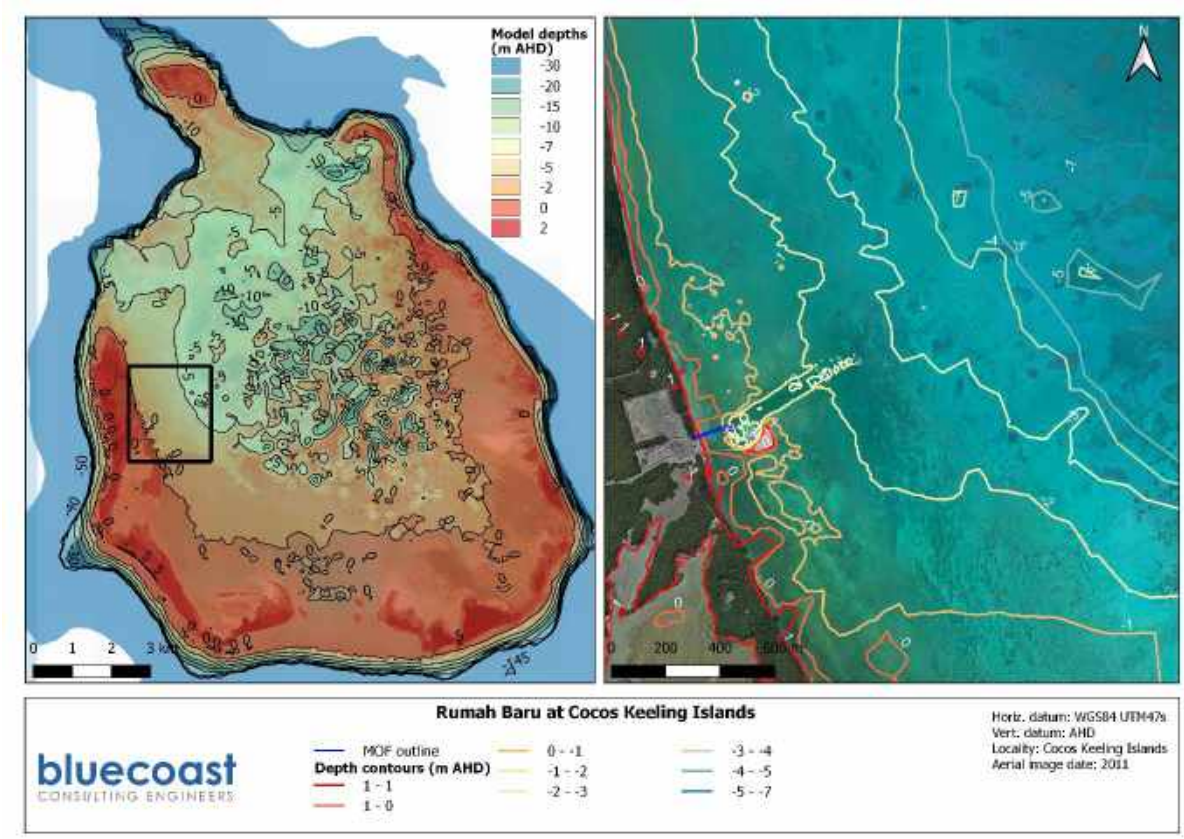

Figure 12: Bathymetry over the entire atoll out to 50m depth (left) and the localised bathymetry at Rumah Baru with seagrass beds visible in the nearshore areas (right).

3.2.2 MOF designs

Two design options for the MOF structure were considered in this analysis. Both options have a similar layout, location (see Figure 1) and extent but differ in the structure type. The first option is a solid structure, constructed of geotextile sand containers in a similar fashion to the existing ferry terminal. This option is displayed in Figure 13. The second option is a piled design, as displayed in Figure 14. This second option allows for the largely unhindered movement of water and sediment beneath the structure while the solid structure blocks such movements.

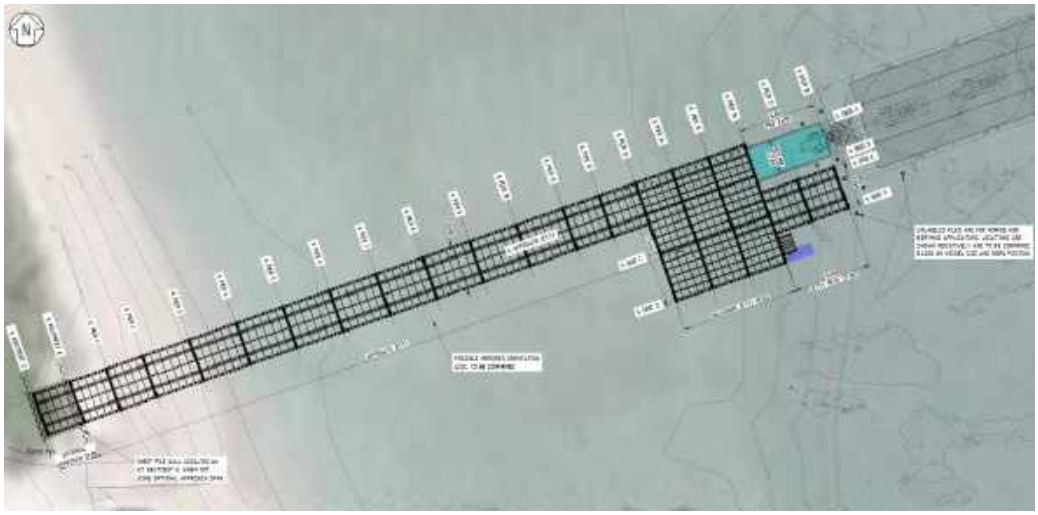

Figure 13: MOF solid design option

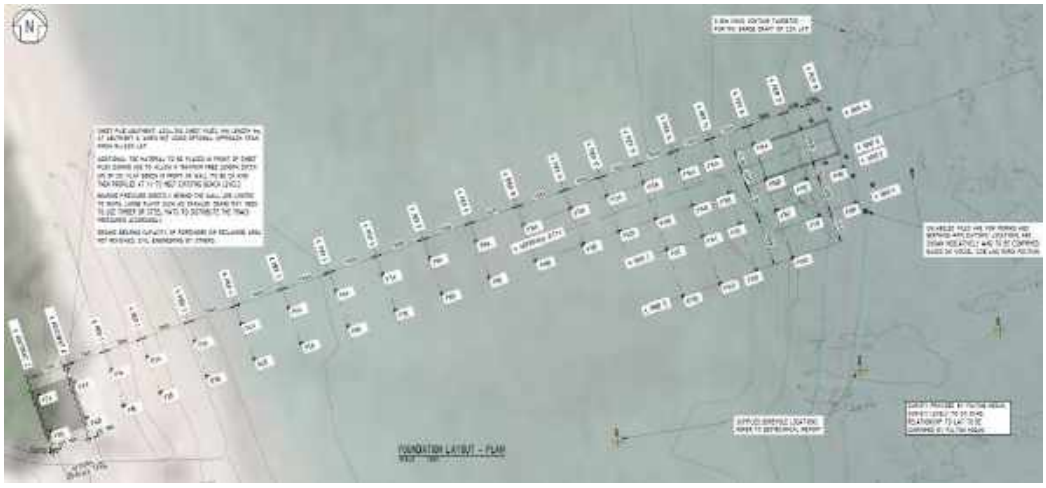

Figure 14: MOF piled design option.

3.3 Local metocean setting

A review of the local metocean settings and analysis of site-specific metocean data has been used to quantify the important processes at the MOF site. This in turn will inform the approach and modelling applied to the impact assessment.

3.3.1 Sea levels

Sea levels at CKI are predominantly tidally driven. Table 10 provides tidal planes for the Home Island tide gauge. The tidal modulation of water levels enables significantly more energy to enter the lagoon at high tide, meaning the state of the tidal cycle has an impact on sediment transport as well as wave energy.

The non-tidal component comprising a range of drivers depending on exposure and location of the coast. Analysis of seasonal and long-term sea level change at the Home Island tide gauge data presented in RHDHV (2018a) shows that:

- there is a significant inter-annual sea level variation of around 100mm above and below mean sea level (MSL) on average;
- during April to September there is typically a negative sea level variation; and
- during October to March there is typically a positive sea level variation.

Extreme sea levels are discussed above in Section 2.5.1.

Table 10: Tidal levels from CKI taken from the Australian National Tide Tables (AHO, 2017)

Tidal plane	Height (m LAT)	Height (m Tide Gauge Zero)
Highest Astronomical Tide (HAT)	1.56	1.73
Mean High Water Spring (MHWS)	1.08	1.25
Mean High Water Neap (MHWN)	0.85	1.02
Mean Sea Level (MSL)	0.66	0.83
Mean Low Water Neap (MLWN)	0.47	0.64
Mean Low Water Spring (MLWS)	0.24	0.41
Lowest Astronomical Tide (LAT)	0.00	0.13

* Data was derived from DoT (2010)

3.3.2 Wind climate

The wind climate at the site displays a distinct seasonality with the highest mean winds occurring in the winter period from July to October and the lowest mean wind energy over the summer period from December to March. Most winds are from the south-east quarter with over 80% of the year coming from the east, south-east or south (see Figure 3). The highest peak wind speeds occur over the period November to March, when cyclones and tropical lows occur. This period is the calmest in terms of mean wind speeds but has short periods of extremely high wind speeds.

3.3.3 Currents

Offshore of the study site (100-200m), the lagoonal currents are predominantly wind driven northerly currents that are parallel to the shore due to the predominant south-easterly wind

direction. There is an occasional reversal in current direction around high tide. Nearshore the current is predominantly south along the shoreline and is induced by swell penetrating the lagoon from the north generating southward littoral drift (HGM,1999b).

3.3.4 Swell and sea waves

Section 2 provides a detailed description of the site wave climate for both day-to-day and extreme conditions. For the purposes of the coastal processes assessment a brief description of the sites wave climate is provided below.

The wind waves (sea with Tp < 8s) at the site are strongly correlated with wind speed. Most sea wave generating winds are from the south-east. Over the winter period there are consistent low amplitude swell waves at the site due to the frequency of large swell events generated by extratropical cyclones travelling from west to east across the southern portion of the Indian Ocean (latitude 35–40°S). The swell arrives at the CKI from the south to south-west and reaches the study site on the lagoon side of West Island through the refraction and diffraction of the swell waves through Western Entrance and Port Refuge to Rumah Baru. Swell waves during summer originate from the less frequent northerly tropical cyclones.

3.3.5 Tropical cyclones

At CKI during low wave energy months of November to March there are also the highest proportion of northerly swells in the lagoon. These northerly swells generated from tropical cyclones and tropical depressions are not frequent and have variable effects. However, they produce the largest swell waves at the site. Although the mean energy of the swell outside the lagoon may be lower over this period, the northerly component means there is less attenuation of swell before it enters the lagoon. The northerly waves also arrive at high oblique angle to the shoreline, driving strong alongshore movement of sand. The historical wind records show the most extreme winds occur in this period and hence also the most extreme wave climate is likely to be generated in the November to March months.

3.4 Changes to local wave climate and currents

3.4.1 Coupled Delft3D FM model setup

Deltares' Delft3D-Flow Flexible Mesh (FM) modelling suite was adopted. The hydrodynamic (D-Flow) and spectral wave (D-Wave) models were used to simulate tidal as well as wind and wave driven currents. These models were originally developed and calibrated by Bluecoast for the coastal inundation and shoreline stability assessments completed as part of the recent coastal vulnerability assessment for Cocos (Keeling) Islands (Bluecoast, 2020).

The Delft3D model was updated to have two way coupling of the waves and hydrodynamics through the duration of a simulation. The two-way couple modelling approach is termed

Flow-Wave-Flow with the water level and currents simulated in the hydrodynamic (D-Flow) model and the wave conditions separately evaluated in the D-Wave module. The effect of waves on hydrodynamics (via radiation stresses, forcing, enhanced turbulence and enhanced bed shear stress) and the effect of hydrodynamics on waves (via set-up, current refraction and enhanced bottom friction) are accounted for within this coupled approach (Deltares, 2015).

The model domain covers the entire southern atoll (see Figure 15) with the resolution increased over the MOF site and surrounds. The bathymetry and elevations are based on the datasets listed in Table 1 and supplemented with and a high-resolution survey of the proposed MOF site taken July 2020. The model setup, utilised datasets and model calibration for the coupled model are presented in Bluecoast 2020 coastal vulnerability assessment. The coupled D-Wave/D-Flow model was forced with tides, winds and waves from the offshore boundary.

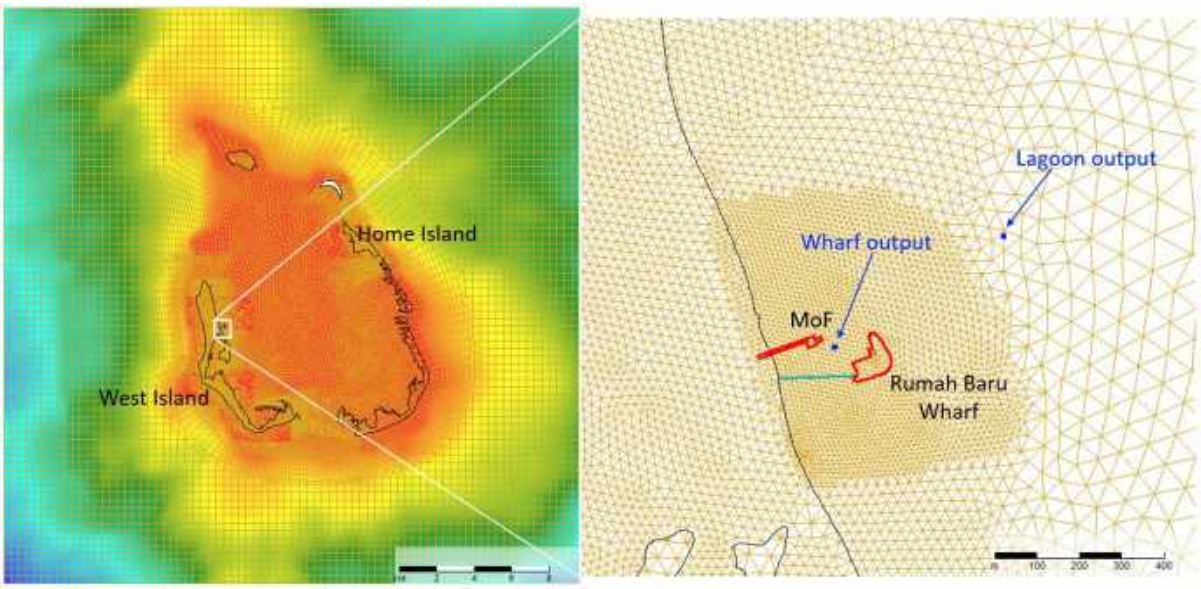

Figure 15: Model domain and bathymetry and key output points of the D-Flow model and the high resolution (12m) area around the MOF site.

3.4.2 Modelling scenarios

To identify the potential changes to tidal, wind and wave induced currents for the solid and piled designs options, three scenarios were simulated:

- base case being the existing conditions based on the 2011 bathymetry with the ferry terminal and associated infrastructure present;
- Solid MOF design option was introduced to the base case; and
- Piled MOF design option was introduced to the base case.

The wind climate at the site displays a distinct seasonality with the highest mean winds occurring in winter and the lowest mean winds occurring over summer. The simulations were run over three periods that were representative of the conditions experienced at the site:

- a low-energy period in summer
- a large south-easterly swell event during a period of high mean winds in winter, and
- a large northerly swell event during the typically low-energy period in summer.

Previous analysis of 12-months of wave and current measurement collected at CKI (RHDHV, 2019) identified a period of low-energy waves in summer on the 5th January 2019 and a large south-easterly swell event in winter on 24th July 2018 (RHDHV, 2018). These periods are representative of the range of conditions expected at the site, with south-easterly swell event occurring in the winter months when the highest mean winds occur and the low-energy events typical of summer conditions. In addition to these periods, modelling of a synthetic 20-year ARI design wind event of 30.5m/s (Table 7) of sustained winds for three hours from a tropical cyclone coming from the north northeast was carried out. The scenario is representative of the rare northerly swell events that usually take place between November to March. The cases are rare yet more severe as northerly events have the longest fetch and the highest potential for sediment transport at the site.

3.4.3 Base case modelling

The base case model included the Ramah Baru ferry terminal island as a solid structure and the piled jetty defined as circular piles with 0.35m diameters within the model domain (Figure 15). Output locations were positioned near to the proposed MOF structure to assess any potential changes to the local wave climate and currents as well as 400m away from the site (Figure 15).

For the base case, resulting maps of current velocities during the peak of the ebb and flood tidal flows are presented as:

- Figure 16 (regional) and Figure 17 (project site) for a typical summer (low- wave energy) wave conditions
- Figure 18 (regional) and Figure 19 (project site) for a large south-easterly winter swell event on 24th July 2018
- Figure 20 (regional) and Figure 21 (project site) for the 20-year ARI northerly event.

The results are described for each period below.

Low energy period (summer)

Figure 16 and Figure 17 show that the West Island side of the lagoon there is a bias of tidal flow entering and exiting the western entrance, resulting in northerly ebb and southerly flood currents. These general lagoon circulation current persist until approximately 200m east of the ferry terminal where a salient feature is evident shoreward of the ferry terminal (Figure 17) (Bluecoast, 2020). Where the site is located, ebb and flood flows (Figure 17) show that within 500m east of the shoreline, currents north of the ferry terminal are moving in a southerly direction along the shoreline driven by the persistent refracted swell waves, with some of the current diverting eastward towards the central part of the lagoon when encountering the dredged channel and existing ferry terminal structures. Circulation currents have speeds less than 0.1m/s at the site but up to 0.3m/s across the lagoon with the largest current speeds of 0.5m/s at the western entrance.

Previous studies found that flow at the shallow entrances at the southern end of the lagoon are predominantly unidirectional flowing into the lagoon and would not impact the site (Bluecoast, 2020). It has been observed that there is erosion of the shoreline downdrift (to south) of the ferry terminal.

Large south-easterly swell event (winter)

During the large south-easterly swell event in July 2018 (Figure 18 and Figure 19) the ebb and flood currents are also southerly directed along the shoreline but larger in magnitude. Under these conditions an eddy forms north of ferry terminal on an ebb tide. Current magnitudes along the oceanward side of West Island reach 1.2m/s, driven by the south-easterly swells. At the MOF site the restriction of southerly flow caused by the ferry terminal and jetty piles is evident on the peak ebb tide. In Figure 18 it is evident that the lagoon circulation act in the opposing direction, however the net direction is determined by the swell waves.

Rare northerly swell event (20-year TC winds in summer)

Base case modelling of the rare but more severe northerly events presented in Figure 20 and Figure 21 show that wave driven circulation dominates. Tidally induced currents only showing a slight reversal out the lagoons western entrance on an ebb tide. During a flood tide, current speeds to the south reach approximately 0.5m/s through the entrances and 0.3m/s near the project site (see ‘Wharf output’ on Figure 15) due to the wave and tidal induced currents all going into the lagoon. As swell waves from this direction have the longest fetch and therefore largest currents, the highest potential for sediment transport at the site also occurs during these rare events.

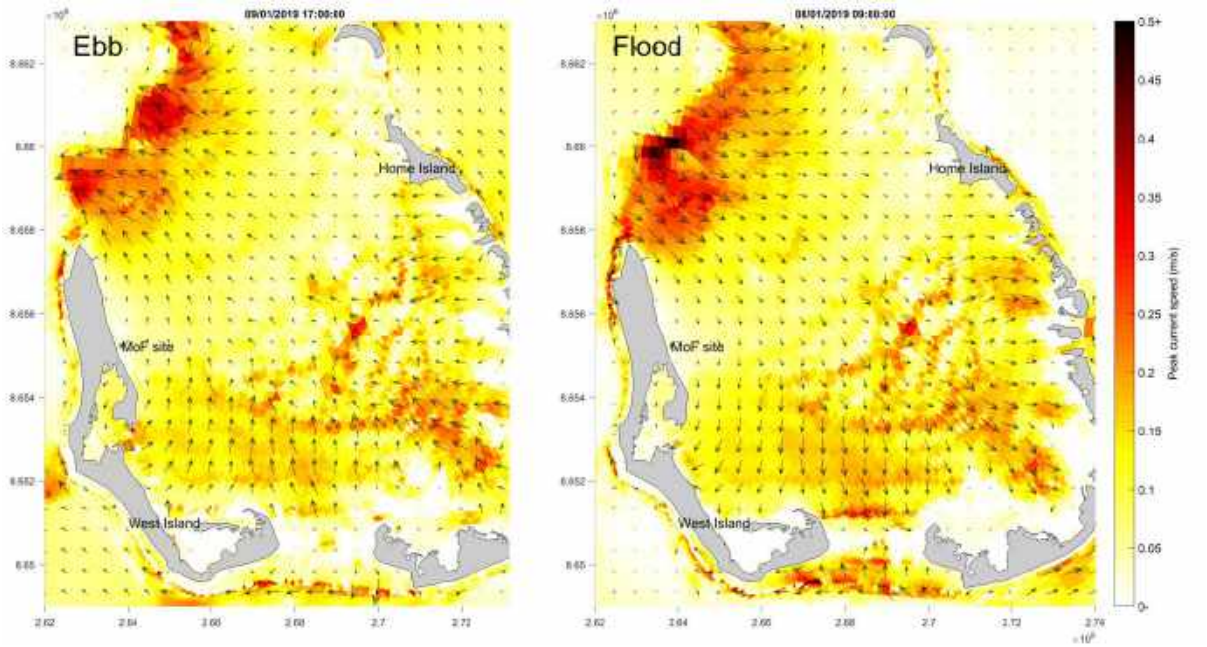

Figure 16: Current speeds and direction around Cocos Island during peak ebb (left) and peak flood (right) tide during a period with low-energy wave conditions on 5th January 2019.

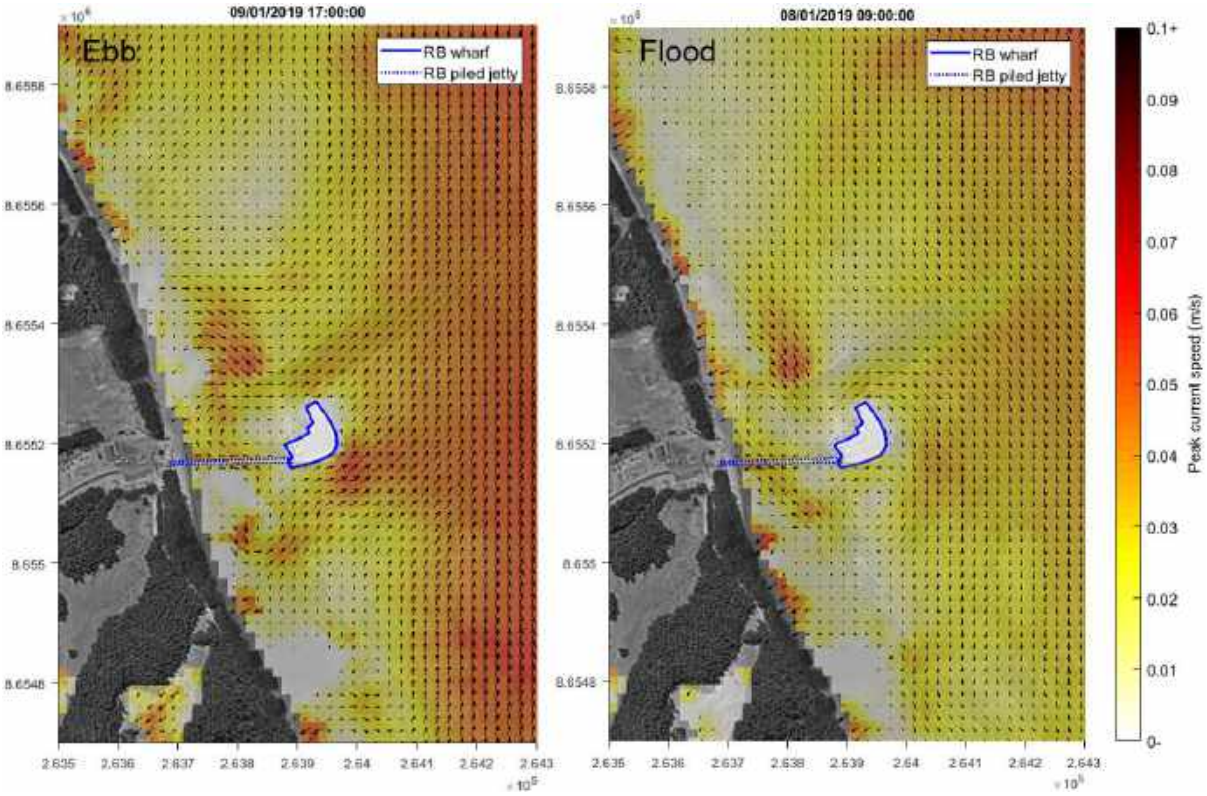

Figure 17: Current speeds and direction at the MOF site during peak ebb (left) and flood (right) tides for a low-energy wave condition (5th January 2019).

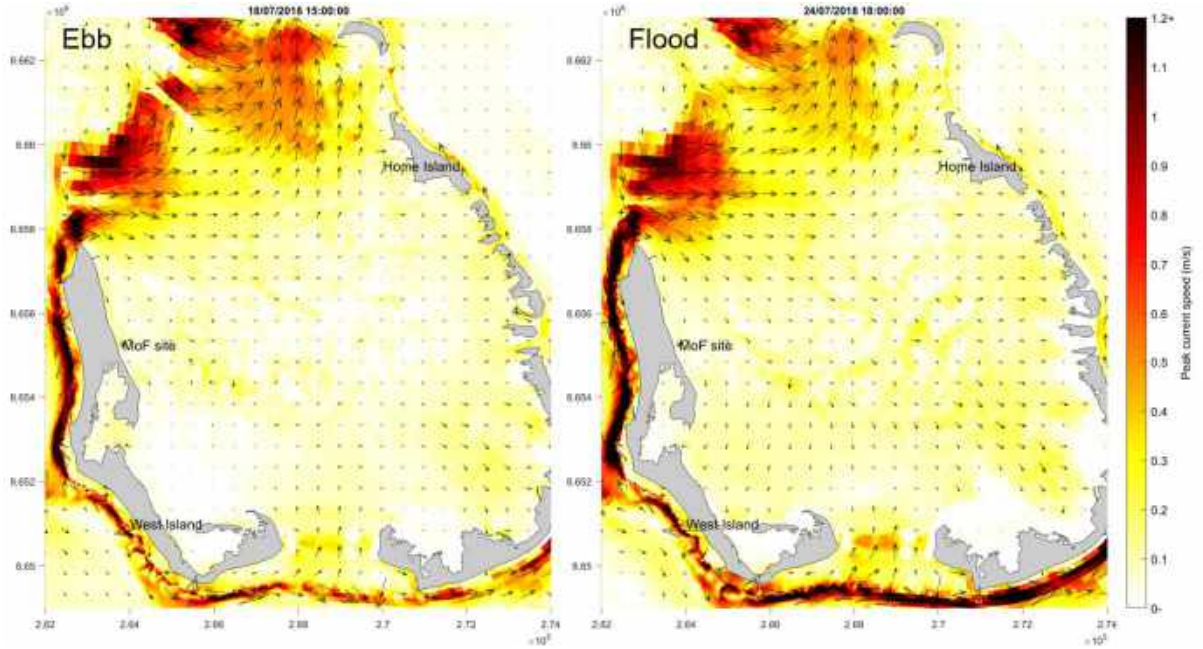

Figure 18: Current speeds and direction around Cocos Island during peak ebb (left) and peak flood (right) tide during a south-easterly swell event on 24th July 2018.

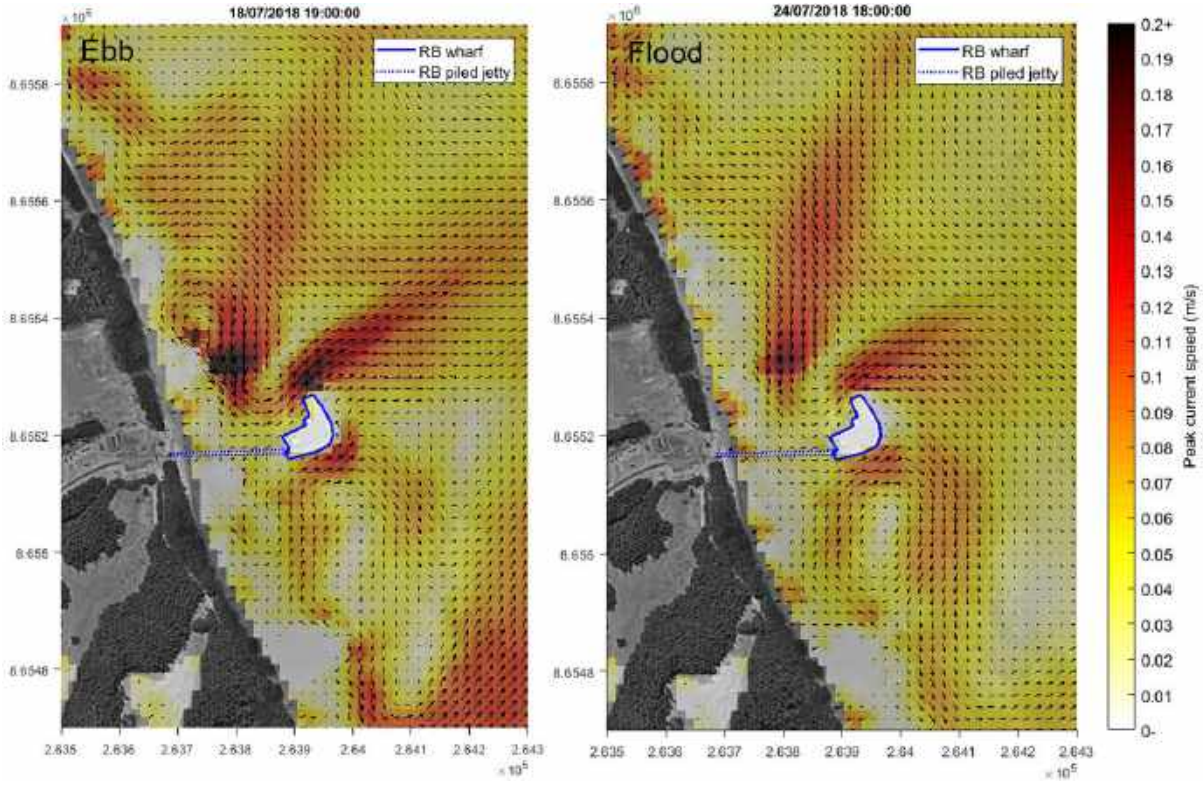

Figure 19: Current speeds and direction at the MOF site during peak ebb (left) and peak flood (right) tide during a south-easterly swell event on 24th July 2018.

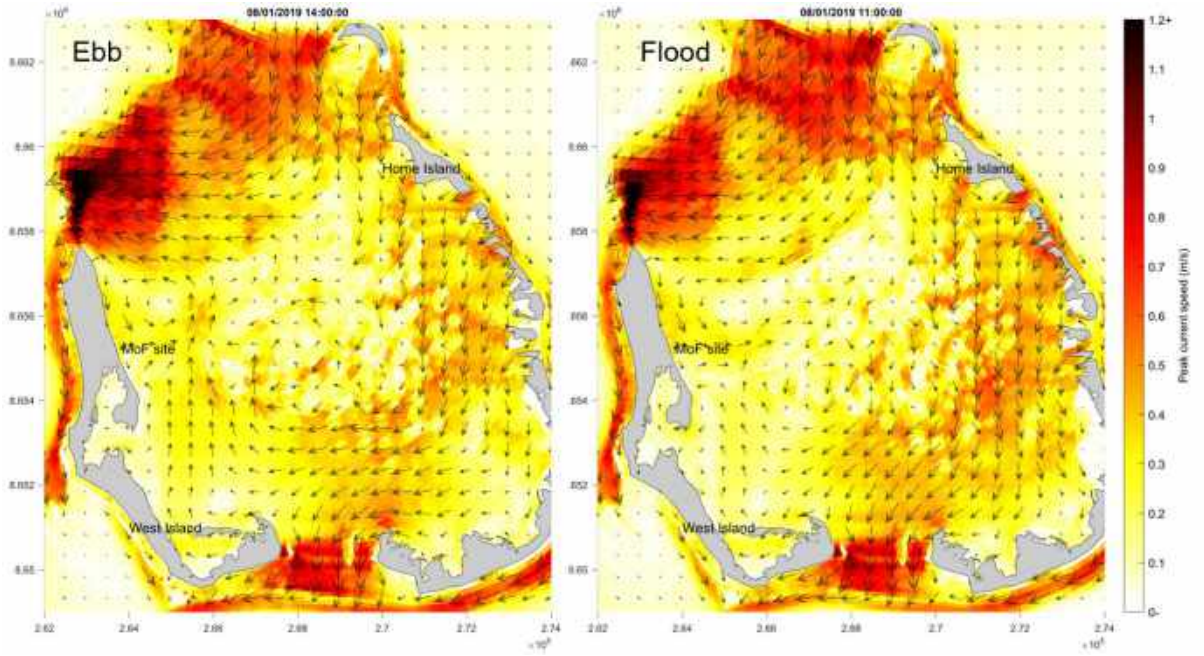

Figure 20: Current speeds and direction around Cocos Island during peak ebb (left) and peak flood (right) tide during a synthetic 20-year ARI northerly swell event in summer.

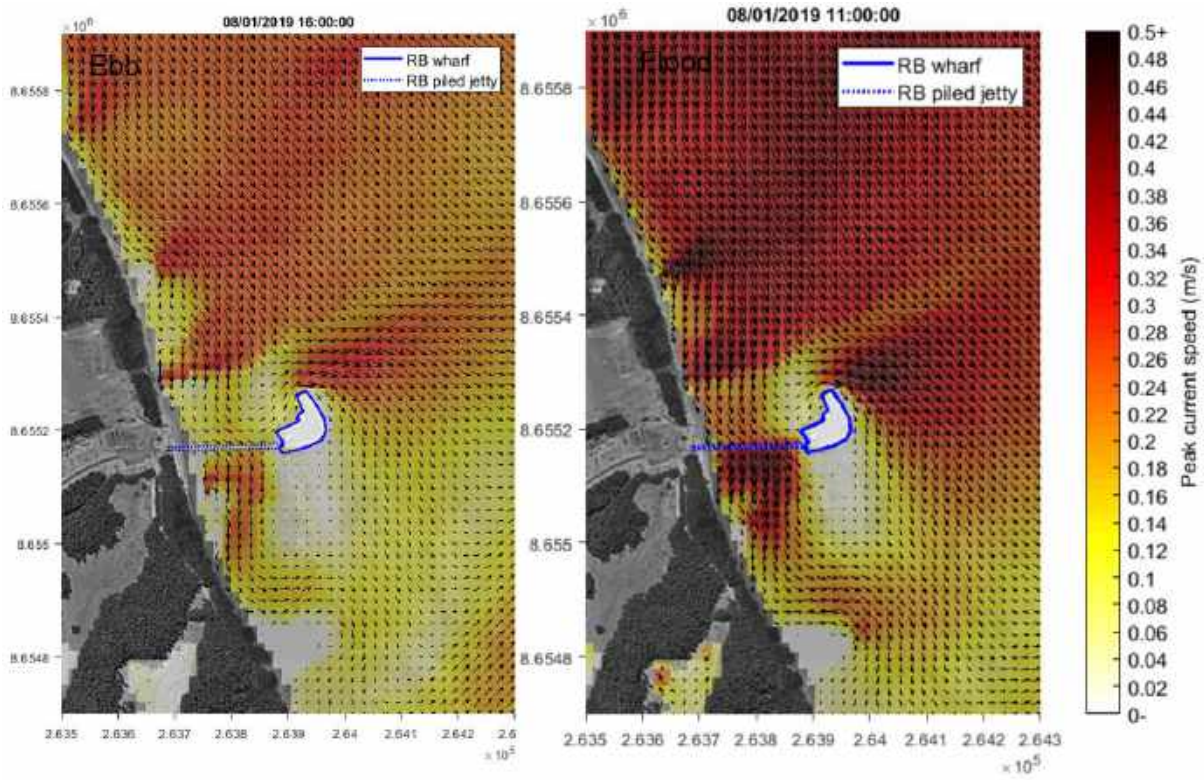

Figure 21: Current speeds and direction at the MOF site during peak ebb (left) and peak flood (right) tide during a synthetic 20yr ARI northerly swell event in summer.

3.4.4 MOF design options modelling

The two design options were schematised into refined Delft3D FM models and simulation completed for the three selected periods described above. The solid structure was represented as a complete blockage in both the flow and wave models. The piled design was modelled as circular piles with 0.61m diameter in the flow model (not represented in the wave model due to grid resolution). For the scenarios, timeseries and relevant current statistics for the MOF wharf area and maps of mean current speeds are presented as:

- For the simulations during low wave energy period,
    - timeseries for the wharf output are shown in Figure 22 and Table 11 shows the relevant current statistics at the wharf and lagoon outputs (locations see Figure 15)
    - Mean current speeds and directions over the simulation period are compared for the base case and the two design options in Figure 23.
- For the simulations during a large south-easterly swell event,
    - timeseries at the wharf output and relevant current statistic are presented in Figure 24 and Table 12 respectively.
    - Mean current maps for the base case and two design options in Figure 25.
- For the rare northerly swell event,
    - Figure 26 shows the timeseries at the wharf output and Table 13 the relevant current statistics at the wharf and lagoon outputs.
    - The mean current maps are displayed in Figure 26.
- Current difference plots in Figure 27 showing differences in mean current speeds between the base case and the solid MOF design for the three simulation periods. ‘

The results are described for each period below and summarised in difference plots.

Low wave energy period (summer)

As in the base case analysis in Section 3.4.3, currents are mostly south-easterly to southerly with the dominant pathway southward along the shoreline. Peaks in current speed at the output location coincide with the periods of higher wave heights. During higher water levels there is a small reduction in current speed between the base case and solid MOF design and minor difference between the base case and piled MOF design.

Wave heights are reduced with the solid design by approximately 0.05m with no notable difference between the base case and piled design. Changes to current direction were most notable at low tides with the base case weighted mean direction of 114°N and for option 2 122°N. The average flow within the Rumah Baru area is reduced by the solid MOF structure. For both options and over all scenarios, there was no change to currents and waves at the lagoon output 200m from the site.

Large south-easterly swell event

With the solid MOF design, current magnitudes are reduced by approximately half for the average and maximum at the wharf output. Current directions shift from eastward to south-easterly. Only minor changes are evident between the base case and solid MOF design for this period. For the base case and option 2, southward currents flowing towards the site are high at the edge of the dredged channel and reduce over the channel creating an area of potential deposition when the current slows over the deeper area. The solid structure in solid MOF design shows a reduction in currents northward of the MOF location and moves the area of lower current speeds north of the structure.

Rare northerly swell event (20yr TC winds)

The model scenario had the largest mean current speeds and the highest potential for sediment transport at the site. Unlike in the previous scenarios, the solid MOF design runs in solid MOF design saw an increase in current speeds at the wharf output. The largest differences are in the direction of the current at the wharf output, which shifted from 108 °N to 173 °N for solid MOF design. Current maps show the solid design diverting currents from the northerly swell wave off the front of the structure. Figure 27 shows there are minor changes to the mean currents between the base case and piled MOF design.

Difference between options

Differences in mean current speeds are compared between the base case and solid MOF design for the three simulation periods. There was very little differences between base case and the piled MOF (i.e., maximum difference of 0.01m/s) so this comparison has not been shown. The difference maps display a positive change (red) when there is an increase in mean current speeds from the base case to design option and a negative change (blue) when a decrease in mean current speeds is modelled.

The low energy period shows approximately 0.02m/s reduction in current speeds at the structure. During the large swell event there was a reduction of approximately 0.07m/s around the structure and an increase in 0.07m/s for the northern tip of the solid design. The 20year ARI northerly storm event changes were larger in magnitude, with a 0.08m/s reduction and increase over a larger area around the structure head and at the northern tip of the design respectively. The reduction in the structure shadow may lead to deposition of sediment north of the structure that has been transported south down the West Island lagoon coastline with the prevailing currents. As well as changes to sediment transport pathways, there is the possibility of disturbing seagrass beds and altering the coverage of these habitats with changes to currents seen in solid MOF design.

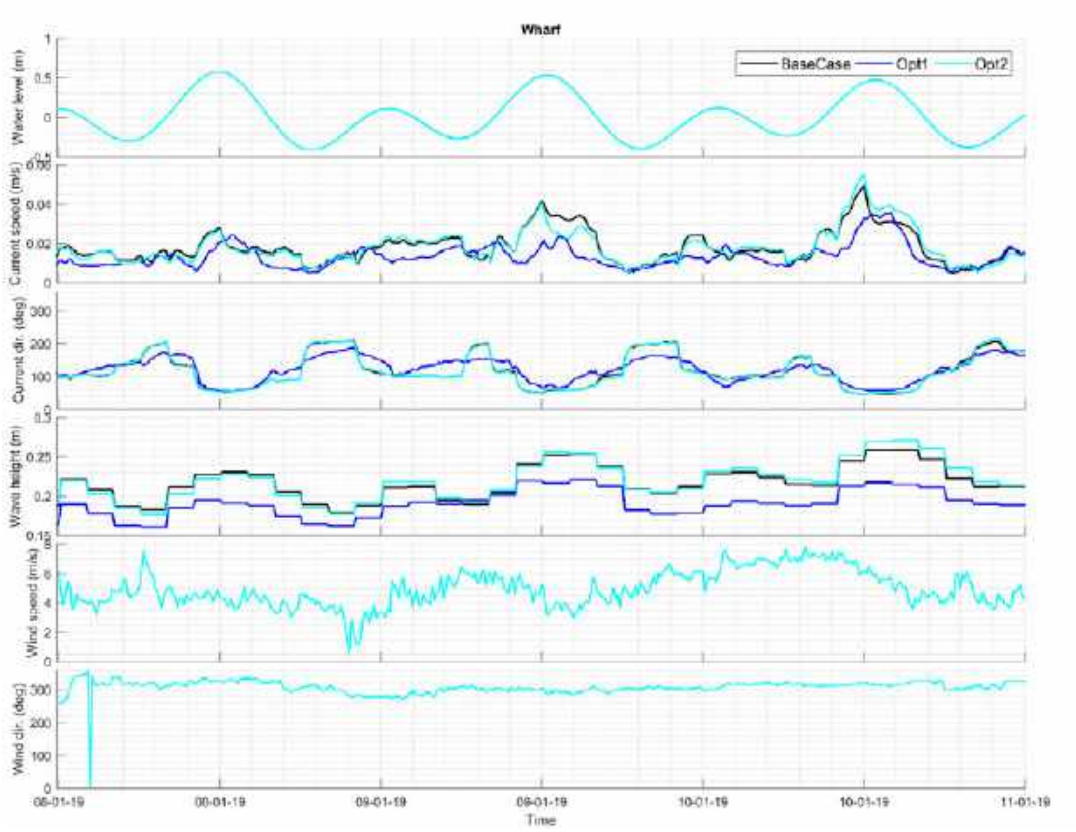

Figure 22: Comparisons of water levels, current speeds and direction, wave heights and winds at the wharf output location over the three model setups of base case, solid MOF design (solid) and piled MOF design during a period with low-energy wave conditions on 5th January 2019

Table 11: Current statistics for the wharf and lagoon model observation points during a period with low-energy wave conditions on 5th January 2019.

Model output locations	Model setups	Current magnitude (m/s)				Current direction (°N)
		Mean	50th %ile	95th %ile	Max	Net mean
Wharf	Base case	0.02	0.02	0.03	0.05	114
	Solid MOF design	0.01	0.01	0.02	0.04	122
	Piled MOF design	0.02	0.02	0.04	0.06	113
Lagoon	Base case	0.04	0.03	0.07	0.08	27
	Solid MOF design	0.04	0.03	0.07	0.08	26
	Piled MOF design	0.04	0.03	0.07	0.08	28

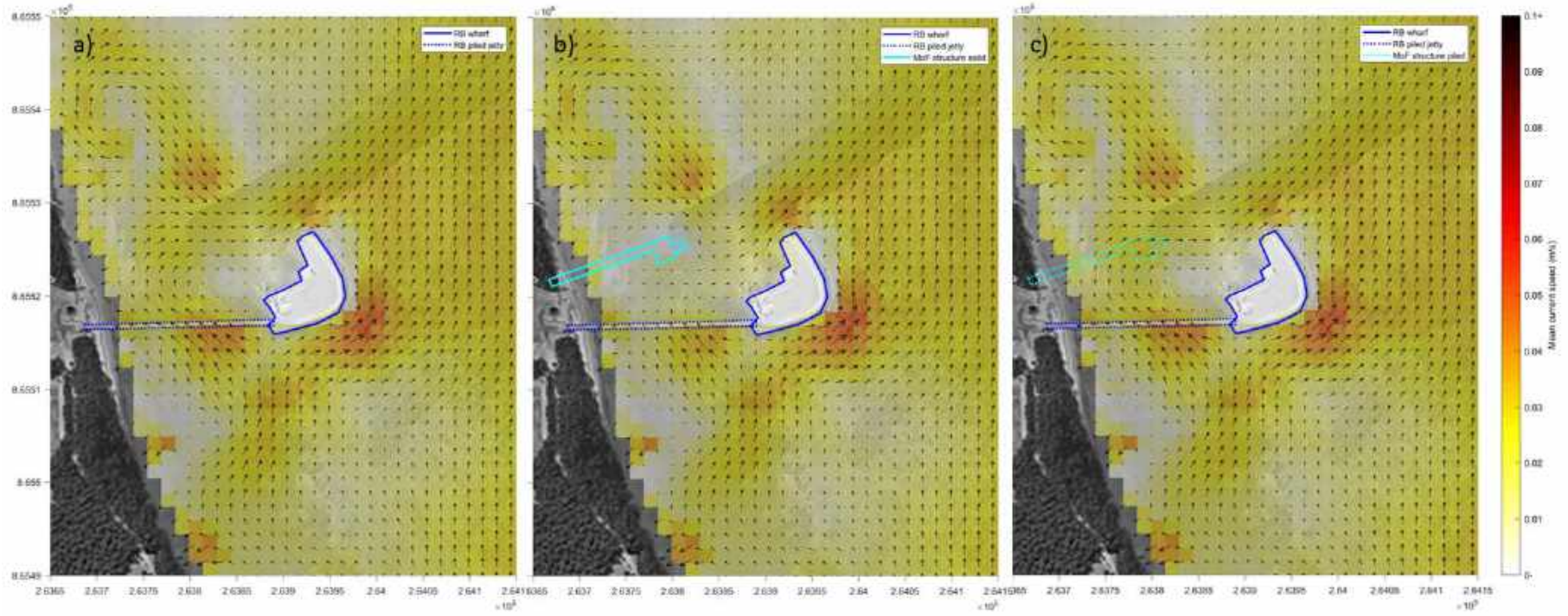

Figure 23: Mean current speeds and direction at the MOF site over the simulation period for (a) base case, (b) MOF solid design option and (c) MOF piled design option during a period with low-energy wave conditions on 5th January 2019.

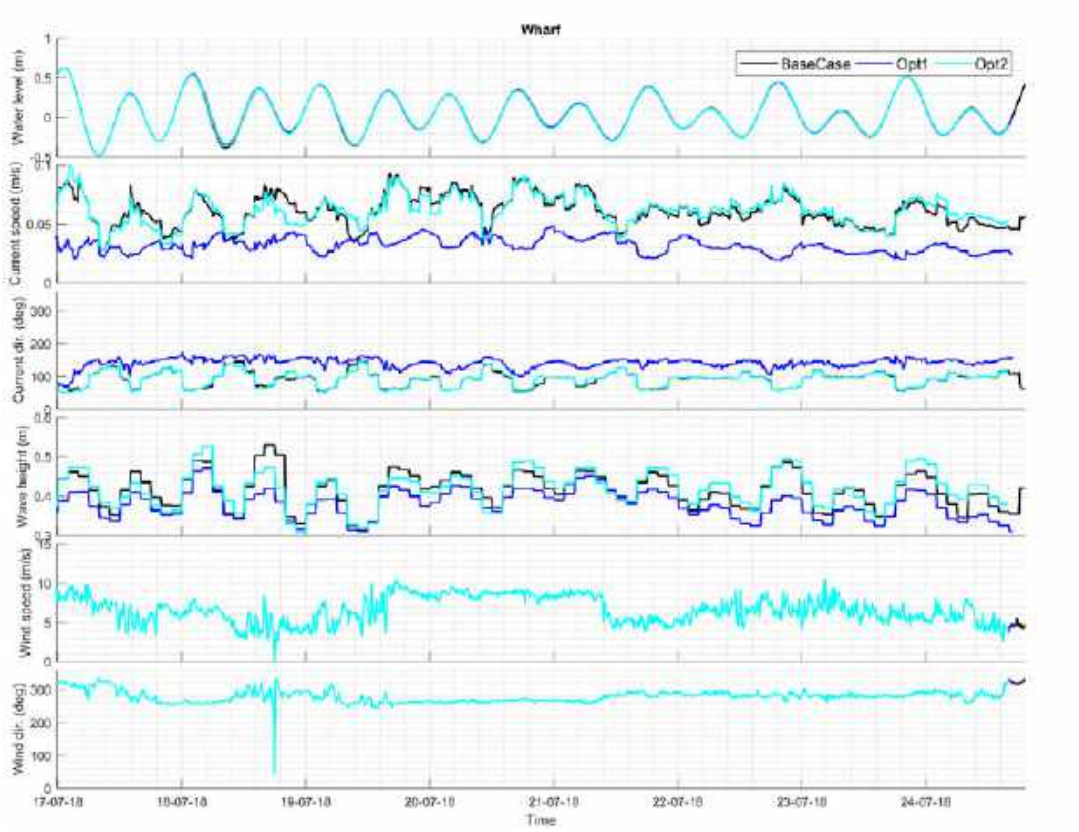

Figure 24: Comparisons of water levels, current speeds and direction, wave heights and winds at the wharf output location over the three model setups of base case, solid MOF design (solid) and piled MOF design during a south-easterly swell event on 24th July 2018.

Table 12: Current statistics for the wharf and lagoon model observation points during a south-easterly swell event on 24th July 2018.

Model output locations	Model setups	Current magnitude (m/s)				Current direction (°N)
		Mean	50th %ile	95th %ile	Max	Net mean
Wharf	Base case	0.06	0.06	0.08	0.09	92
	Solid MOF design	0.03	0.03	0.04	0.05	142
	Piled MOF design	0.06	0.06	0.08	0.10	92
Lagoon	Base case	0.07	0.07	0.09	0.10	64
	Solid MOF design	0.07	0.07	0.09	0.10	65
	Piled MOF design	0.07	0.07	0.09	0.10	64

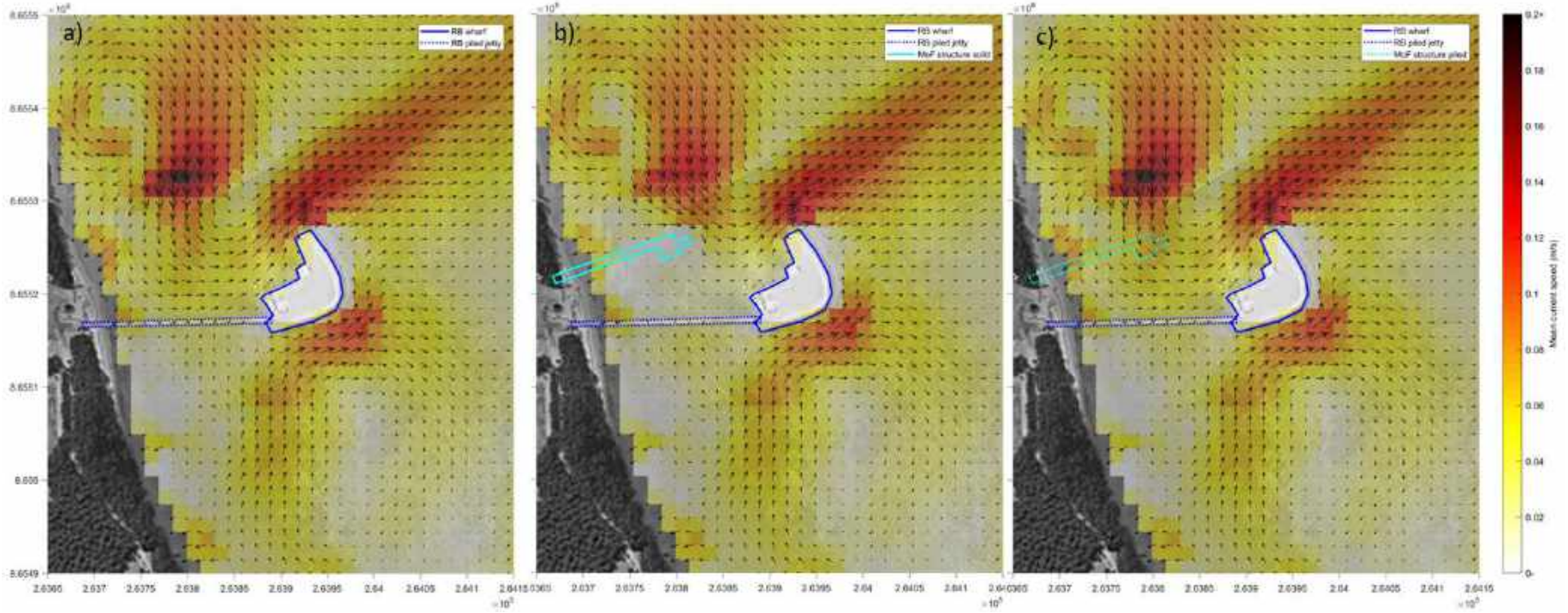

Figure 25: Mean current speeds and direction at the MOF site over the simulation period for (a) base case, (b) MOF solid design option and (c) MOF piled design option during a south-easterly swell event on 24th July 2018.

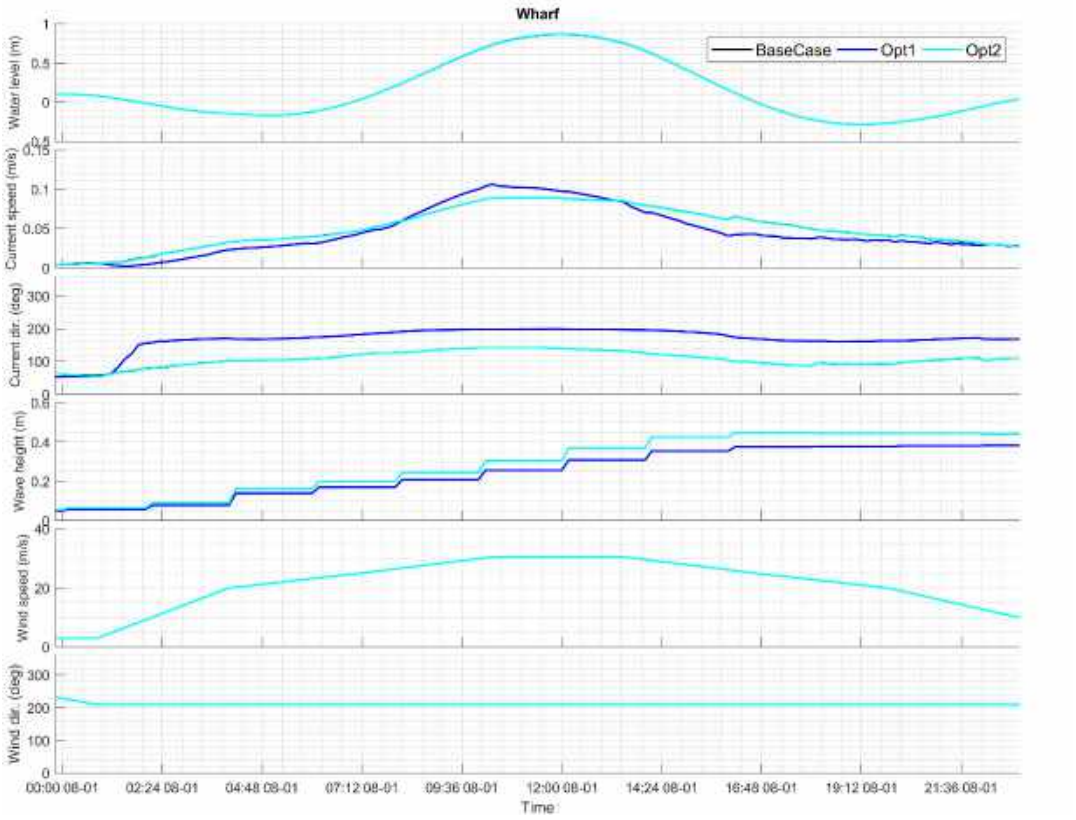

Figure 26: Comparisons of water levels, current speeds and direction, wave heights and winds at the wharf output location over the three model setups of base case, solid MOF design (solid) and piled MOF design during a synthetic 20yr ARI northerly *swell event in summer.*

Table 13: Current statistics for the wharf and lagoon model observation points during a synthetic 20yr ARI northerly swell event in summer

Model output locations	**Model setups**	**Current magnitude (m/s)**				**Current direction (°N)**
		Mean	**50th %ile**	**95th %ile**	**Max**	**Net mean**
Wharf	Base case	0.05	0.05	0.09	0.09	108
	Solid MOF design	0.05	0.04	0.10	0.11	173
	Piled MOF design	0.05	0.05	0.09	0.09	108
Lagoon	Base case	0.18	0.20	0.29	0.30	111
	Solid MOF design	0.18	0.20	0.29	0.30	111
	Piled MOF design	0.18	0.20	0.29	0.30	111

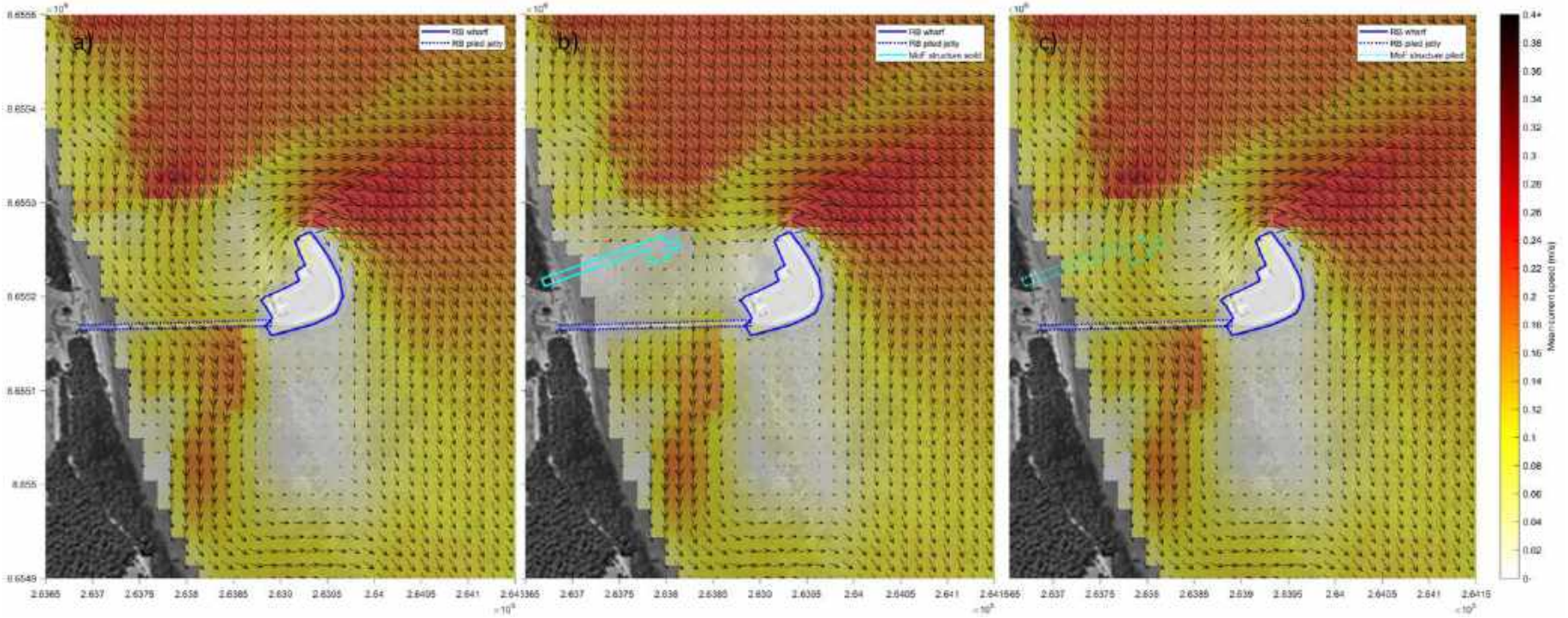

Figure 27: Mean current speeds and direction at the MOF site over the simulation period for (a) base case, (b) MOF solid design option and (c) MOF piled design option during a synthetic 20yr ARI northerly swell event in summer.

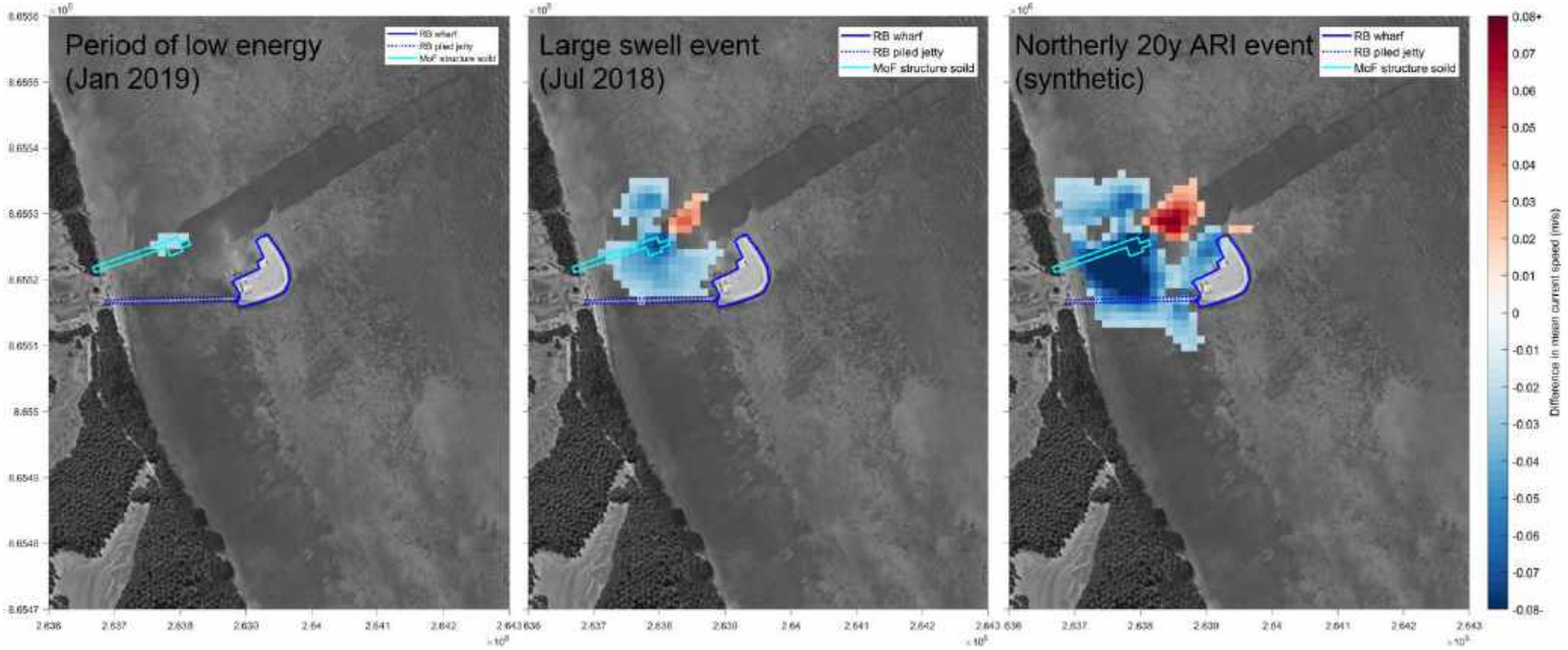

Figure 28: Difference in current speed between solid design and base case during a period of low energy (left), during a south-easterly swell event (middle) and during a synthetic 20yr ARI northerly swell event in summer (right) where positive difference is an increase in current speeds with the inclusion of solid MOF design.

3.5 Sediment transport and shoreline change

3.5.1 Preamble

Longshore sediment transport is the process of sand or other sediments moving in an alongshore direction and is driven by waves arriving oblique to the shoreline orientation. As evident in the current modelling in Section 3.4.3, the locally generated lagoon wind waves and lagoon circulation act in the opposing direction. However, the net current direction is southerly is determined by the swell waves. The net direction of alongshore sediment transport around the entire West Island was determined from a range of sources as part of the detailed work Bluecoast completed on the Cocos (Keeling) Islands – Coastal Vulnerability Report for WA DPLH. The net direction of alongshore sediment transport along the project site is also in a southerly direction.

3.5.2 Alongshore sediment transport at the project site

At the proposed MOF site, the inshore sediment transport is largely driven by northerly swell; and secondary is the south-easterly wind waves resulting in a net southward transport along the shoreline. The low-energy environment and the potential for sand transport both southwards with swell and northwards with wind waves makes it difficult to predict the effect of a beach crossing structure on sand movement (HGM, 1999b). The tidal modulation of water levels enables significantly more swell energy to enter the lagoon at high tide, meaning the rate of sediment transport is a function of tidal cycle state as well as the magnitude of the swell waves.

Previous seasonal analysis in rates of sediment transport at the site show that the potential for greatest transport in the over single events occurs in the November to March period due to northerly swell effects, this period also has the lowest mean rates of transport due to low energy (HGM, 1999b). While the period where the most consistent sediment transport rates occur in July to October due to the constant high-energy wind and swell climate (HGM, 1999b). Operational swell waves at the MOF site transformed from CAWCR data in Section 2.4.2 display this seasonality at the site. Table 3 shows that mean swell waves during the November to March (Summer) period have the lowest mean wave heights of 0.11m but the highest maximum of 0.69m. Hence both winter and summer conditions favour southerly sand movements along the project shoreline.

As part of the design investigations for the Rumah Baru ferry terminal, two temporary groynes were constructed at the study site. Their objective was to determine the direction of the net longshore sediment transport as well as the volume (HGM, 1999b). The temporary groynes were constructed in July 1999 and were 32 metres in length and located 20 metres either side of the boat ramp. After construction a substantial amount of sand was observed to have built up against the northern side of the northern most groyne. During a spring tide

with higher tidal ranges some of the sand on the northern side bypassed the groyne at the landward end. Figure 29 shows the cumulative change in the beach volume profiles over the period where the northern side of the northern groyne had a net increase in subaerial beach profile volume of 0.86 m^3/m, which predominately occurred over a 3-day period around 18 August 1999 (RHDHV, 2018b). The short-term findings indicated a southerly alongshore sediment transport. However, as the structures failed in August and there are no longer term observations from the trial (HGM, 1999b).

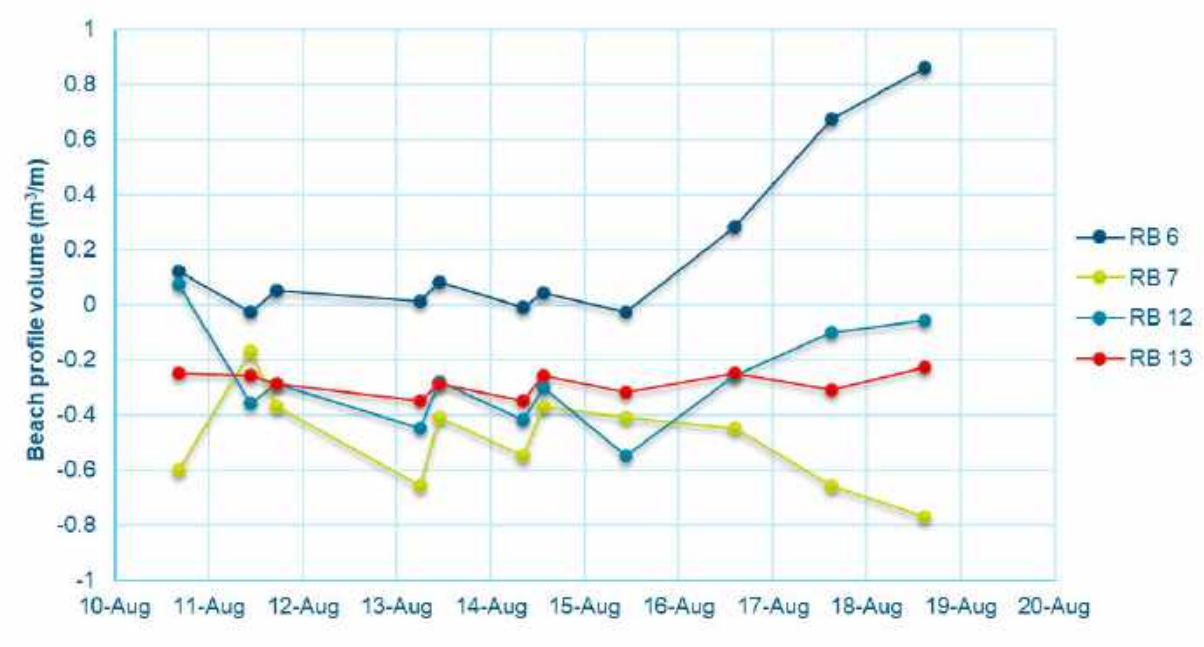

Figure 29: Cumulative change in beach profile volume at Rumah Baru foreshore during 1999 temporary groyne trial. Note: RB 6 is 1 m to the north and RB 7 is 1 m to the south of the northern groyne. RB12 is 1 m north and RB13 is 1 m south of the southern groyne (RHDHV, 2018b)

The most tangible evidence of the net southerly alongshore transport comes from the maintenance required to regularly clear sand from the boat ramp. This boat ramp was designed to allow sand movements but has tended to act as a groyne and requires regularly clearing. The Shire periodically remove sand from the ramp area and stockpiled in the carpark or used it directly for other works around West Island. Available records are documented in Table 14. The records indicate that accumulated sand is removed at a rate of approximate 1,200m^3/yr. Given sand is known to build up and bypass the boat ramp both over the top and seaward of the structure, this rate of removal is only representative of part of the total alongshore transport rate. Instances of sand removal in Table 14 are more frequent over winter when the refracted swell waves are more energetic. Some permits noted sand build up after northerly wind events in keeping with the modelling of waves in Figure 10 and currents from northerly events in Figure 21 and Figure 27.

Table 14: Shire of Cocos Keeling Island excavation permit records for sand removal from the boat ramp area at Rumah Baru.

Date	Cubic meters (m^3) removed	Reason for permit/comment
8/5/2017	150	Clearing boat ramp
10/5/2017	157	Clearing boat ramp
11/10/2017	150	Clearing boat ramp
8/11/2017	195	Clearing boat ramp
20/12/2017	150	Clearing boat ramp and emergency sandbags on Airforce Road
3/7/2018	126	Clearing boat ramp after northerly wind
5/7/2018	150	Clearing boat ramp after northerly wind
31/7/2018	180	Clearing boat ramp and emergency protection
16/8/2018	229	Clearing boat ramp
15/10/2018	144	Clearing boat ramp
8/11/2018	169	Sandbags needed at Trannies Beach
6/12/2018	90	Clearing boat ramp
17/1/2019	165	Sand replacement at West Island playground
Total	**2,055**	**Rate of sand removal from boat ramp area over 1.70 years was 1,212m^3/yr**

3.5.3 Existing shoreline and historical shoreline change

Following the construction of the new ferry terminal the Rumah Baru shoreline has behaved differently to the adjacent lagoon shores with a salient feature inshore of the island terminal and erosion downdrift (to south). Aerial photography and vegetation line position information spanning a 32-year period, from 1987 to 2019, was available for West Island and Home Island. The vegetation lines were used as an indicator of shoreline position, particularly the upper part of the beach and/or the barrier vegetation. Close inspection and comparison of

these images and vegetation lines reveals the long-term changes to beach planform within the study area. The estimate accuracy is approximately five meters. Vegetation lines available for analysis are displayed in Figure 30. The vegetation line in the Rumah Baru area can be defined as 'stable or accreting' within the selected analysis area. The accreted shoreline is in the lee of the ferry terminal. Just further south from the analysis area, the shoreline is eroding (see Figure 31).

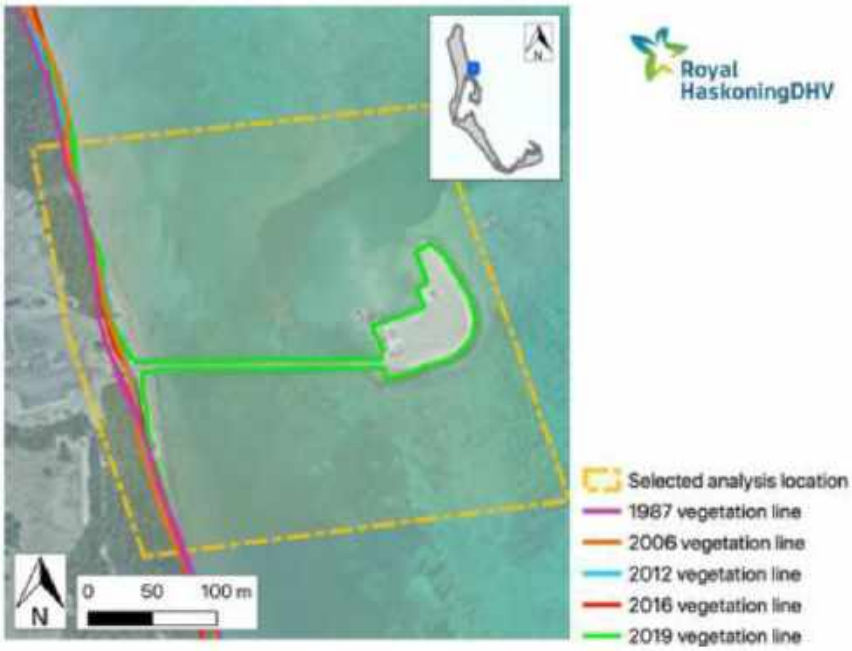

Figure 30: Historical vegetation lines at the Rumah Baru port facility (source: Bluecoast 2020)

Beach to the north of ferry terminal.

Looking north from the ferry terminal jetty with boat ramp in the foreground and sand stockpile in the background.

Large mature tree to south of ferry terminal threathened by on-going erosion.

Eroding shoreline to the south of the mature tree.

Figure 31: Photos of Rumah Baru.

3.5.4 Shoreline change due to designs

Shoreline change because of the two MOF designs was investigated. Under current conditions the shoreline inshore of the ferry terminal is stable or accreting (Figure 30), while the shoreline to the south is eroding. Any changes in the alongshore sediment supply is detrimental to the atoll shorelines which are highly vulnerable to change (Bluecoast, 2020). The shoreline south of the structure depends on the supply of sediment from the net southward transport.

The solid MOF design represents a 100% blockage of the north to south sediment transport pathway, with significant impacts expected as:

- Accumulation of sand on the northern (updrift) side shortly after construction. If this sand is not mechanically bypass around the structure, the sand will start to move seaward, along the northern edge of the MOF with the potential to infill the dredged channel at the end of the MOF jetty.
- Numerical modelling showed that the solid design resulted in changes to the currents at the site. The change currents due to the presence of the solid MOF is likely to further promote deposition of lagoon sediments in the dredged channel and berthing area.
- Downdrift (south) of the solid MOF structure the shoreline will erode following construction. This part of the lagoon shoreline is already eroding and further alongshore sediment starvation would accelerate this shoreline retreat with the potential of a breach into North Lagoon.

The piled MOF design will allow most of the sand to move under the structure with an estimated reduction in alongshore sediment transport of only 5-10%. This will have much

less of an impact on the sediment supply to the south and associated shoreline change. Enhanced infilling on the dredged channel is unlikely with the piled MOF design as it will not trap sand on the updrift side.

3.6 Wrack accumulation

A historical issue at the site is wrack accumulation which is produced by a combination of biological and physical processes. The lagoon seabed is densely covered in seagrasses. With the stronger winds, wrack[1] accumulates on the downwind beaches. During the dry season (July to October) the strong trade winds can lead to wrack accumulation along the project shoreline. Residence of West Island have also observed large wrack accumulation between November and March when reduced flushing of the lagoon (lower winds) as well as a potential seasonality in the growth rates and increase in productivity of the plants in the warmer water with higher irradiance (HGM, 1999a & Larkum, 1989).

Under the solid MOF design, wrack would tend to build up on the foreshore against the southern side of the solid structure (see Figure 23) and potentially within the dredged basin, requiring regular maintenance or screening. Wrack accumulation is not expected to be a significant issue with a piled MOF design. It is noted that this was one of the main reasons a piled option was selected for the design of the Rumah Baru jetty. Difference maps (Figure 28) showing changes to current magnitudes with the solid MOF design structure may also disturb the seagrass bed and suspend more of the material, especially during low tide when the seabed currents are stronger. Mean current differences for piled MOF design showed no changes larger than 0.01m/s between the piled design and the base case.

[1] 'wrack' being the term used to generally describe the organic matter that washes up on beaches.

4 References

Bluecoast, 2020. Cocos (Keeling) Islands coastal vulnerability study: coastal vulnerability assessment report (volume I). Report prepared for Department of Planning, Lands and Heritage, February 2021.

Deltares, 2015. D-Flow Flexible Mesh: D-Flow FM in Delta Shell. user manual. Deltares systems. Version: 1.1.148.

Larkum A.W.D., McComb A.J., & Shepherd S.A, (eds) 1989. Biology of seagrasses. Elsevier, Amsterdam. 841 pp.

Halpern Glick Maunsell (HGM), 1999a. Rumah Baru environmental investigations: progress report 9, September 1999.

Halpern Glick Maunsell (HGM), 1999b. Investigations for the proposed freight and passenger facilities at Rumah Baru (Cocos Islands): 1999 annual report physical processes

RHDHV, 2018a. Additional Task 1 - Post-event report: 24th July 2018 swell event. Report prepared for DPLH as part of the Cocos (Keeling) Islands Coastal Vulnerability Assessment

RHDHV, 2018b. Data Gathering and Desktop Review. Report prepared for DPLH as part of the Cocos (Keeling) Islands Coastal Vulnerability Assessment.

RHDHV, 2019. Task 5 – Metocean data collection report. Report prepared for DPLH as part of the Cocos (Keeling) Islands Coastal Vulnerability Assessment